NTNU

Norwegian University of
Science and Technology

Kick detection using downhole weight measurements

Alberto Joseph Cheru

Petroleum Engineering
Submission date: August 2017
Supervisor: Sigve Hovda, IGP

Norwegian University of Science and Technology
Department of Geoscience and Petroleum

Acknowledgement

Foremost, we would like to express my profound gratitude to my supervisor, Associate Professor Sigve Hovda for his tireless supervision, guidance, valuable suggestions and remarkable interest which paved a way to the accomplishment of this thesis.

My sincere thanks are due to EnPe-NORAD, and Statoil under Angolan Norwegian Tanzanian Higher Education Initiative (ANTHEI) project for financial support throughout my studies. Also I highly appreciate the support from the University of Dar es Salaam (UDSM), at the Department of Chemical and Mining Engineering (CME) for hosting and allowing me to use their facilities during my thesis work.

Last but not least, I would like to express my heartfelt and special appreciations to my family members for their prayers, moral support and guidance they provide to me in my life and throughout my studies. My parents, Mr and Mrs Joseph Cheru are real the best mentors I can ever have in my life.

Abstract

Drilling optimization is a key tool for a company which wants to achieve the best drilling performance and ultimately low effective drilling cost. In achieving these, use of correct weight on bit(WOB) as part of drilling optimization is inevitable in order to achieve an optimal rate of penetration. Not only that weight on bit is important in optimizing drilling performance, but also can be used to quickly anticipate the downhole conditions using downhole weight on bit measurements.

This thesis presents kick detection models based on different drilling parameters which are directly related to weight measurements especially downhole weight on bit. The drilling parameters which were highly considered in modelling are mud weight and buoyancy factor. In the analysis on how these parameters may change during drilling operation, the mathematical models were subjected to different factors including gas fraction, bottomhole pressure, temperature and cuttings concentration in the well. All these factors were found to affect mud weight and buoyancy factor and gas fraction was found to have high impact on mud weight and buoyancy factor. Well geometry and drill string geometry were also taken into account in developing mathematical models which take into account geometry of the drill string. Two models were developed including the Law of Archimedes model and the Force – Area model. The two models were used to calculate the hookload at the surface and it was determined that both give approximately the same results of surface hookload with the Archimedes model being more accurate.

Finally, mathematical models for mud weight and buoyancy factor which use downhole weight on bit were developed. It was revealed that the analytical torque and drag model can simply be used to calculate downhole weight on bit from surface weight measurements. Dependence of weight on bit on wellbore friction was taken into account. The torque and drag model was used to calculate downhole weight on bit using real time drilling data from well 47 – 8 – 5. Computer program was created to iteratively simulate hookload values to match the measured hookload. The simulation was found to give hookload values close to measured values which were then converted into bulk density and buoyancy factor. Bulk density and buoyancy factor calculated from surface hookload values were found to be sensitive to change in downhole weight on bit and drill string weight thus indicating that downhole weight on bit if calculated accurately can predict the onset of gas kick.

Table of Contents

List of Figures

List of Tables

1.0 Introduction

Influx is an undesirable flow of formation fluid into the wellbore that is below the kick tolerance(Aadnoy & Kaarstad, 2006; Gupta et al, 2013; Hollman et al, 2016). This fluid invasion (oil, natural gas, or water) into the well from the formation happens mainly as a result of underbalance condition which occurs when the bottomhole pressure becomes less than the formation pore pressure.

Kick is defined as the volume of influx that exceeds kick tolerance that cannot be safely circulated out of the well(Hollman et al, 2016). Sometimes kick, especially gas kick can enter into the wellbore due temporary reduction in hydrostatic pressure caused by swabbing or by drilling into the formation that contains gas even with a suitable overbalance(Gupta et al, 2013; Jonathan Felipe Galdino et al, 2013) and very rarely, by drilling into neighbouring producing wells(Skalle, 2015b).

It is important that kick is detected as early as possible to avoid getting into an uncontrollable amount of influx which ultimately results into hazardous blowouts and/or loss of life and equipments. For this reason, early kick detection, without which, kicks would become more difficult to handle is of paramount importance.

Detecting kicks earlier helps to take necessary measures in controlling them with the proper kick handling techniques without causing any hazardous event such as formation damage(Velmurugan et al, 2015). In a normal situation, a gas kick is removed by circulating the well using surface adjustable choke(Rader et al, 1975).

According to Swanson et al (1997), early kick detection is of crucial importance in slimhole wellbores and small annular volumes are required to maintain integrity of the well, which means that allowable kick volumes must be small.

A number of kick detection techniques have been developed and implemented. However, the increase in complexity of well drilling operations poses the need for early, more accurate and more reliable kick detection methods because more deep water drilling operations with increasing tight pressure margins have significantly increased,Velmurugan et al (2015). Stokka et al (1993) developed a gas kick warner whose working principle is to measure the propagation time of a

pressure pulse travelling through the well. This method enables detection of small amounts of free gas in the annulus while downhole.

1.1 Methods Used to Detect a Kick

It is crucial and beneficial to detect a kick at the very beginning and as quickly as possible. Early kick detection can minimize the kick size and reduce the risk of blowout when controlling the well. Due to technology advancement, kick-detection equipments are installed during drilling operations which work on basis of kick indicators. There are a lot of kick indicators but the following are the most important kick indications(Ling et al, 2015):

1. Pit gains due to the increase in the mud return flow rate

Mud is circulated outside the well to the surface and is taken to the mud pit via the mud return line. Observing level of the mud in the pit may help to notice the change in mud volume especially increase in mud flow. This increase in mud flow is called pit gain and is the difference between mud inflow volume and the mud outflow volume given as $\mathrm{Pit_{gain}} = \mathrm{V_{in}} - \mathrm{V_{out}}$. This method has its drawback because the reliability of pit gain depends on size of the mud pit and the larger the mud pit the slower the gain in the pit volume is and the less accurate this method becomes.

2. Mud flows when pumps are off

The common practice to confirm that there is occurrence of kick in the well is to switch of the pumps and look at the flow. Mud flowing while the pumps are off sends a message that there is an extra energy pushing the mud out of the well. This might be the fluid flowing into the well due to formation pressure being high than the bottomhole pressure. This method may be reliable but it seems less quick as it may be the last indicator before deciding whether it is the real or fake kick.

3. An increase in the mud return flow rate

Increase in mud flow rate can be used as a simple method to anticipate the onset of influx in the well. When increase in mud return flow rate is observed at the surface, the main reason is influx at the bottom caused by high pressure fluid, normally a gas. This influx sets an additional flow on the mud displacing the denser mud as the gas keeps flowing into the well. However, sometimes this may not be the case as well breathing(ballooning) may also be the reason for increase in mud flow rate. Ballooning is the situation where the well releases back the mud that was taken by the

formation and may sometimes be confused with the kick. This drawback makes this method less reliable as it can sometimes give a false information.

4. Gas cutting or salinity changes in the drilling fluid

Gas cutting is the crucial method to use in detecting the onset of a kick. It is the measure of how much has is present in the mud to the total volume of the mud. This parameter affects many factors like mud weight, surface weight and buoyancy factor all of which have interrelated to each other. Gas cutting is sometimes known as gas fraction and its works fine depending on the type of mud used. In the oil based mud this method may be less quick, because more gas is likely to be absorbed than in the water based mud. If a water based mud is used and with the system to monitor change in gas fraction in the well, then looking at other parameters associated with gas fraction may be a quicker way to anticipate the occurrence of the kick.

5. An increase in drill string weight

Change in drill string weight is normally associated with the condition down the hole. If mud weight is decreasing, the main reason might be increase in mud weight leading to a corresponding decrease in buoyancy factor which ultimately affects the weight of the drill string at the surface. On the other, increase in weight of the string may be the result of increase in buoyance factor which is caused by mud weight being lowered from its original value. This is because there is a direct relationship between density of the mud and buoyancy factor and this relationship will be discussed in detail in the next chapters.

6. An abrupt increase in rate of penetration (ROP)

This method can be used to indicate the occurrence of a kick by paying attention to the change in rate of penetration. Rate of penetration is the increase in bit depth per hour an is measured in meters drilled per unit hour. Change in rate of penetration indicates in increase in differential pressure which is the difference between the pore pressure and hydrostatic pressure due to mud column in the annulus expressed as difference in equivalent densities (i.e. $\rho_{pore} - \rho_{mud}$). Assuming other factors remain constant and the mud weight is unchanged, then increase in rate of penetration indicates increase in pore pressure. The same conclusion can be drawn that if the pore pressure

remains constant, an increase in penetration rate indicates the decrease in mud weight which might be caused by the mud being cut due to an influx of a low density fluid, normally a gas influx (Skalle, 2015b).

1.2 Sources of Kick in the Well

A kick can occur when mainly when borehole pressure (BHP) drops to below the formation pore pressure. This may happen due to the following reasons:

1.2.1 *Gas/Water Cut Mud*

If gas or salt water contaminates the drilling mud, the average density of the drilling fluid is lowered. This mud weight reduction may sufficiently lower the hydrostatic bottomhole pressure because it depends on density of the mud. Gas contamination has big impact on lowering mud weight than water(Rommetveit et al, 2003)

1.2.2 *Insufficient Mud weight*

Insufficient mud weight means mud weight which cannot provide a sufficient pressure over the formation pore pressure at the bottom of the well at a given depth. This leads to underbalanced condition at the bottom of the well which may result into influx of the low density fluid.

1.2.3 *Improper fill-up*

This may happen when the drill pipe (DP) is pulled out of the hole (POOH) and the hole is not refilled with a sufficient mud to take the space of the drill string pulled out of the hole. If the fluid cannot fill the volume of the drill string, the level of the mud in the annulus which may fail to maintain the bottomhole pressure over formation pore pressure.

1.2.4 *Swab & heave effect*

Swabbing may create swab pressure leading into an abrupt lowering of bottomhole pressure to below the formation pore pressure if a certain volume of mass/steel is removed from the hole too fast. This may be due to tripping out too fast or caused by the effect of heave when the drill string is in slips on a floating drilling unit. The reduced pressure created may be sufficient to allow fluids to enter the wellbore.

1.2.5 *Lost Circulation*

Due to presence of fractures in the fresh formation and under overbalanced condition, drilling mud may be lost into the formation through the fractures or thief zones. If this is more severe, reduction

in mud-column sufficiently to drop the mud hydrostatic pressure below the pore pressure may occur thereby initiating a kick(Aadnøy, 2006).

1.2.6 *Gas diffusion*

When drilling using Oil Based Mud (OBM) in deep and high pressures and temperatures wells, gas un expectedly diffuse and get dissolved completely in the base oil of the mud. This may occur even when drilling in an overbalanced condition. The gas stays dissolved and it is circulated upwards with the mud and when it reaches the pressure and/or temperature conditions favorable for its expansion, a quick and sudden out flow of mud mixed with gas erupts at the surface especially for high pressure and high temperature wells (Rommetveit et al, 2003)

2.0 Modelling of a Gas Kick

Modelling of gas kick aims at developing mathematical models that can be used to predict the onset of a kick in the wellbore. The models that take in every possible parameter which is likely to be affected by influx is developed. The models are developed based on whether the well is vertical or deviated. In discussing the mathematical models, different parameters are considered including gas fraction, cuttings concentration, temperature, pipe rotation, pressure and more importantly buoyancy factor.

2.1 Current Methods used in Calculation of Buoyancy Factor

In calculation of buoyancy or buoyancy factor, two approaches are normally used in calculating weight of the drill string in the wellbore. The two approaches include the Archimedes law and piston force approach. The Archimedes law states in simplicity that the buoyancy equals the weight of the displaced fluid. The piston method on the other hand is the uniaxial force balance applied to each geometrical change in the string(Aadnoy & Kaarstad, 2006; Aadnoy et al, 1999). According to Aadnoy et al (1999), if both of these methods are used correctly, they provide identical results and on top of that, Aadnoy et al (1999) keeps arguing that the Archimedes principle can be used for all cases.

2.1.1 *The Generalized Law of Archimedes*

According to Archimedes principle, buoyancy of the body is equal to the weight of the displaced fluid in which it floats. On the other hand, this implies that buoyancy is the force acting opposite to the gravitational weight of the body which acts downwards. It is therefore concluded in the work by Aadnoy & Kaarstad (2006), that only pressure contributes to buoyancy and this pressure acts on the projected vertical area. It is important to first understand the direction of gravitation so that the projected area can be easily determined. For instance, if the gravitation acts in the z direction, then buoyancy acts in the orthogonal plane x, y. The buoyancy force F(z) can then be determined using:

$$F(z) = P(z)A(z) \tag{2.1}$$

Where $P(z)$ is the hydrostatic pressure at the given depth and $A(z)$ is area upon which the pressure acts and is given by $A(z) = \int_x \int_y dx\, dy$. Equation(2.1) is the general equation for buoyant force and can be applied to any geometry of the body. For instance, if this equation is applied to an arbitrary body, say a vertical cylindrical prism shown in Figure 2-1 of height h, the buoyant force F_b, is equal to the difference between bottom and top forces acting on the prism given as $F_b = F_{bottom} - F_{top}$. This force is also equal to the hydrostatic pressure given by $P(z) = \rho gz$, times the projected area (Aadnoy & Kaarstad, 2006).

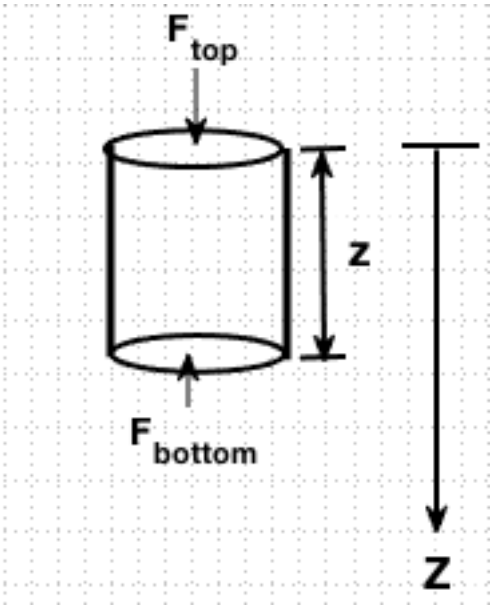

Figure 2-1: Forces acting on the submerged body

2.1.2 *The Force – Area Method (Piston Method)*

The piston method is based on force balance by considering forces acting throughout the drill string. For drill string components (pipes etc.) with different outer diameters connected to form the drill string, an area is exposed wherever there is change in size of the drill string components. The forces acting on the drill string at these exposed areas are equal to the hydrostatic pressure times the exposed area at the particular point of interest. Carefully and proper application of this method gives the same weight of the drill string at the surface in spite of the fact that the forces at the depths may be slightly different(Aadnoy & Kaarstad, 2006; Aadnoy et al, 1999).

2.2 Buoyancy Factor, β

Buoyancy factor is the mathematical expression which defines the effect of the fluid on the submerged body. This effect is called buoyancy and refers to the effect by which the body submerged in the fluid experiences a weight reduction due to an upward force (up thrust) acting, The buoyancy effect which is expressed in terms of buoyancy factor, β depends on density of the fluid in the wellbore, ρ_{mud} and the density of the material, ρ_{steel}, Glomstad (2012).

2.3 Derivation of Buoyancy Factor

The idea behind buoyancy factor is based on the fact that when the body is submerged into the fluid it will measure less than its actual weight following to the famous law of Archimedes. This weight is called the apparent weight of the body and the ratio between the decrease in weight to the actual weight of the body is known as buoyancy factor. This can be mathematically expressed as difference between actual weight W_a, of the body and its apparent weight W_{ap}, divided by its actual weight.

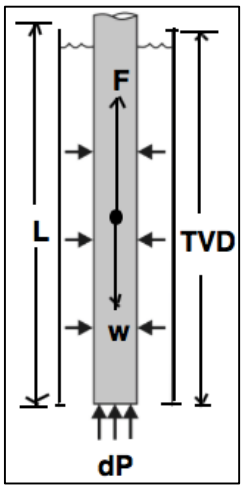

Figure 2-2: Drill pipe submerged in a vertical well(Aadnoy & Kaarstad, 2006)

Figure 2-2 illustrates the drill pipe submerged in a vertical well. The weight in air W_a, of the drill pipe is given by the product of its density ρ_{steel}, the volume of the pipe V_{pipe} = AL, and the gravitational constant g, as $W_{air} = \rho_{steel}$ .A.L.g where A and L are the cross sectional area and length of the pipe respectively.

Suspending the drill pipe into the borehole filled with a fluid with a density ρ_{mud} provides a lift due to hydrostatic force acting at the bottom end of the pipe(Aadnoy & Kaarstad, 2006). This force is equal to the bottomhole pressure multiplied with the cross sectional area A, as $F_{hyd} = \rho_{mud}$. g. TVD. A. The net weight is given by the difference between the pipe weight in air and the buoyant force due to hydrostatic pressure. This net weight which is also known as the buoyed weight of the pipe and is given by:

$$W_{buoyed} = W_{air} - F_{hyd} = (\rho_{steel} - \rho_{mud})gAL \tag{2.2}$$

Where for the case of vertical borehole, L is the same as the true vertical depth, TVD. This buoyed weight W_{buoyed}, is defined as the product of the buoyancy factor β, and the pipe weight in air as $\beta.W_{air} = W_{buoyed}$, which upon substitution of the definitions of W_{buoyed} and W_a gives:

$$\beta.\rho_{steel}.A.L.g = (\rho_{steel} - \rho_{mud})gAL \tag{2.3}$$

Rearrangement and simplification gives the final equation for buoyancy factor as given in (2.4). This equation if used to estimate the weight at the of the drill string gives a correct estimate(Hovda, 2017).

$$\beta = 1 - \frac{\rho_{mud}}{\rho_{steel}} \tag{2.4}$$

Equation (2.4) gives the buoyancy factor on a body submerged in the fluid. Considering the drill string with fluids inside and outside of the drill pipe(s), this equation becomes the simplest form of the buoyancy factor model. The simplifying assumptions include similar inside and outside diameters through the drill string and the same densities inside and outside the drill string.

2.4 Factors Affecting Buoyancy Factor in the Wellbore

In discussing the mathematical models, different parameters are considered including mud weight, gas fraction, cuttings concentration, pipe rotation, side forces and well geometry

2.4.1 *Mud Weight*

Weight reduction due to buoyancy is mainly influenced by mud weight. The uplifting force due to buoyancy changes with the change in density of the mud and a denser fluid reduces the effective

weight of the drill string pipes. A lighter mud on the other hand increases the buoyancy factor hence reducing the uplifting effect of the drilling fluid consequently leaving the weight almost unaffected. This direct relationship between mud weight and buoyancy factor can be deduced from the hydrostatic pressure, P_{hyd} at a depth h in the well as given in equation as:

$$P_{hyd} = g\, h\, \rho_{mud} \tag{2.5}$$

Equation(2.5) suggests that the lower the mud weight, the lower the hydrostatic pressure at a given depth. Combining equation(2.4) and equation(2.5), the relationship between buoyancy factor and hydrostatic pressure can be obtained.

$$\beta = 1 - \frac{P_{hyd}}{g\, h\, \rho_{steel}} \tag{2.6}$$

Many factors can lead to increase or decrease of the mud weight, so does to buoyancy factor. These include gas entering the mud, cuttings in the mud, pressure and temperature, Kristensen (2013). The effective mud weight of the drilling fluid can be estimated by taking into account these factors and is called fluid mixture density or cut mud density,ρ_{mix} (Skalle, 2015a).

2.4.2 *Gas Fraction*

Presence of gas in the drilling fluid reduces the density of the mud. Gas is a very light fluid and occupies large volume due to its ability to expand. When gas enters the wellbore, it mixes with the fluid and gets dissolved into the mud depending on the mud type.

In oil based mud, a small gas kick dissolves into the mud leading to a small increase in volume as the dissolved gas behaves as a liquid. In water based mud, the gas kick does not dissolve and hence a small kick volume expands rapidly with time. The overall effect of the gas cut is lowering of the mud weight and the more the gas into the mud, the lower the mud weight becomes.

The fluid mixture density, ρ_{mix} of the mud depends on the amount of gas which is proportional with gas fraction, C_{gas}. The gas fraction is given as a ratio of volume of the gas, V_{gas} to the total volume of the fluid mixture V_{mix} as given in equation(2.7)

$$C_{gas} = \frac{V_{gas}}{V_{mix}} \tag{2.7}$$

2.4.3 *Cuttings in the Mud*

Cuttings are drilled solids present into the mud during drilling operation. The presence of cuttings in the mud affects the effective density of the mud and normally an increase in mud weight. Cuttings are classified by particle sizes as coarse, intermediate, mediums, ultrafine and colloidal. Particles greater than 2000 microns are regarded as coarse cuttings, those ranging from 250 – 2000 microns are referred to as intermediate cuttings and medium cuttings range from 74 – 250 microns (Skalle, 2015a).

Most of the drilled cuttings are heavier than density of the mud used. If taken in big fraction by volume, the consequence is increase in density of the mud. It is by far important to have all drilled cuttings being carried out with the mud to the surface but not exceeding the limit so as to maintain the quality of the drilling fluid.

2.4.4 *Drill String Rotation*

Pipe rotation has significant effects on mud rheology as rotation affects the viscosity and density of the mud in an indirect way. As the pipe rotates, the cuttings holding ability of the mud increases. However, this depends on the type of mud system that is being used. According to Ozbayoglu et al (2008), pipe rotation together with other factors have big influence on hole cleaning performance. Rotation of the pipe increases the amount of cuttings suspended in the mud and hence the better the cuttings removal from under the bit. If more cuttings are suspended into the mud, density of the mud increases accordingly.

Experimental study by Ford et al (1990) , pipe rotation affects development of cuttings bed revealed that pipe rotation have insignificant effect on minimum fluid transport velocity if low viscosity fluid is used. In medium to high viscous fluids, pipe rotation influences the minimum fluid transport velocity.

Increasing pipe rotation decreases the minimum velocity required to suspend cuttings into the mud. In the experimental study conducted by Sifferman & Becker (1992), pipe rotation was one of the factors which highly affect cuttings suspension in the mud and that the higher the speed of pipe rotation, the more cuttings are eroded from the cuttings bed.

It was demonstrated using Taylor vortices in Lockett et al (1993) and pointed out that pipe rotation is crucial in removing cuttings and suspending them into the mud. McCann et al (1995) in his study on pressure loss in narrow annuli concluded that increase in pipe rotation increases pressure loss especially in a turbulent fluid flow regime and vice versa is for lamina flow regime. Also a similar conclusion was drawn by on pipe rotation that there exists a positive relationship between pipe rotation and pressure drop such that the higher the speed of pipe rotation the higher the pressure drop. Saasen (1998) observed that pipe rotation aids to transport large volumes of cuttings when polymerized water based mud is used.

All these observations infer that pipe rotation indirectly affects the density of the mud in the same manner as it does to cuttings transportation efficiency. Increasing hole cleaning efficiency suggests that more cuttings are carried with the mud. This concludes that mud weight will increase because more cuttings are present into the mud. On the other hand, increase in pressure loss due to pipe rotation as previously discussed signifies reduction in mud weight. This indirect effect of pipe rotation might be due to lowering of mud viscosity which significantly reduces the ability of the mud to hold more cuttings.

Therefore, pipe rotation affects mud weight in both positively and negatively ways. If other factors are kept constant, then mud weight increases with increase in pipe rotation. On the other hand, mud weight decreases with pipe rotation if effect of cuttings concentration and other factors are kept constant.

2.5 Density of a Mud – gas mixture as a Function of Gas Fraction

Change in volume of the gas phase in the mud – gas mixture with changing temperature and pressure as gas rises up the annulus causes the density of the mixture to change. However, for simplicity, it is reasonable to assume that the volume of the liquid phase does not change with temperature and pressure i.e. the volume of the liquid phase is constant. In this sub - section the mud-gas mixture is treated as a homogeneous fluid for a particular temperature and pressure condition and therefore the density of the cut mud can be derived from the law of conservation of volume and mass as follows. The mass and volume of the mixture, M_{mix} and V_{mix} is simply the sum of the masses and volumes of the two phases as:

$$M_{mix} = M_{mud} + M_{gas}$$

$$V_{mix} = V_{mud} + V_{gas} \tag{2.8}$$

Substitution of the definition of mass in terms of volume and density gives:

$$\rho_{mix} V_{mix} = \rho_{gas} V_{gas} + \rho_{mud} V_{mud} \tag{2.9}$$

Dividing with V_{mix} throughout equation(2.9) gives:

$$\rho_{mix} = \rho_{gas} \frac{V_{gas}}{V_{mix}} + \rho_{mud} \frac{V_{mud}}{V_{mix}} \tag{2.10}$$

But since $V_{mud} = V_{mix} - V_{gas}$ and upon substitution into equation(2.10) gives:

$$\rho_{mix} = \rho_{gas} \frac{V_{gas}}{V_{mix}} + \rho_{mud} \frac{V_{mix} - V_{gas}}{V_{mix}} = \rho_{gas} \frac{V_{gas}}{V_{mix}} + \rho_{mud} \left(1 - \frac{V_{gas}}{V_{mix}}\right) \tag{2.11}$$

Using the definition given in equation(2.7), the ratio of the gas volume V_{gas} to the total volume of the mixture V_{mix} is equal to the gas fraction C_{gas}. Substitution of equation(2.11) into equation(2.7) gives the final equation for density of the gas cut mud ρ_{mix} in terms of gas fraction C_{gas}.

$$\rho_{mix} = \rho_{gas} C_{gas} + \rho_{mud} \left(1 - C_{gas}\right) \tag{2.12}$$

Equation(2.12) gives the variation of mud weight as a function of gas fraction without taking into account that gas fraction varies with time in the well bore. The variation of mud weight as a function of the time due to the dynamic change of gas fraction will be established following to the derivation of gas fraction as a function of time.

3.0 Gas fraction and Mud Weight as a Function of Time

Gas fraction is the amount by volume of gas present in the mud which is expressed as a percent of gas in the total volume of the mud - gas mixture. Equation(2.7) gives the gas fraction as the ratio of the volume of gas in the mud to the total volume of the mud – gas mixture. Gas fraction has a big impact on the effective density of the drilling fluid due to the tendency of gas to expand as pressure decreases. It is therefore important to note that while gas influx leads to decrease in bottomhole pressure, it also creates its possibility to expand as it rises up in the annulus.

Normally, gas expansion occurs when gas is on its way out as the mud circulates and with time the annulus gets filled with gas if proper control over gas expansion is not taken. In this section mathematical model of a gas fraction is developed to understand the behavior of the gas in terms of its fraction in the mud as a function of time the gas is allowed to expand. Assumptions put forward in developing the model include two phase flow during circulating the gas out of the well and that gas obeys the real gas behavior.

3.1 Modelling Gas fraction

Gas fraction is a critical parameter to take into account when evaluating the variation of buoyancy factor in the well during a gas kick. Gas expands as it is circulated out of the wellbore. As the gas expands, more drilling fluid overlying the gas column is displaced causing increase in flow rate in the mud return line. If mud flow rate is used as an indicator of the influx, then the kick is indicated by the sudden rise in the mud flow rate in the mud return line.

Expansion of gas is caused by the decrease of the hydrostatic pressure of the mud overlying the gas column. This gas column is a function of time because, at any time t, the distance moved by the top of the gas column can be estimated using the velocity of the gas. During circulating gas out of the well, gas may behave as dispersed gas bubbles or gas slugs in the mud (Skalle, 2015b).The gas velocity depends on the behavior of the gas in the mud as the gas is being circulated out.

Different literatures and experimental works have been performed and it has been observed that the velocity of the gas phase in the mud is a function of the velocity of the fluid mixture U_{mix} and it was further deduced that this velocity depends on the type of the gas whether it is dispersed gas bubbles or gas slugs(Skalle, 2015b; Skalle et al, 1991). The velocity of the mud – gas mixture, U_{mix}

is calculated from the mud and gas flow rates in the well as $U_{mix}(t) = \frac{q_{mud} + q_{gas}}{A}$. Where q_{mud} is the mud flow rate, q_{gas} is the rate of gas influx and A is the annular capacity. The velocity of the gas is given as:

$$U_{gas}(t) = \begin{cases} 1.2\,U_{mix} + 0.2 & \text{for dispersed bubbles} \\ 1.2\,U_{mix} + 0.4 & \text{for gas slugs} \end{cases} \quad (3.1)$$

The distance moved by the top of the gas is D(t) and can be estimated as a function of time t from when the kick is taken as shown in Figure 3-1

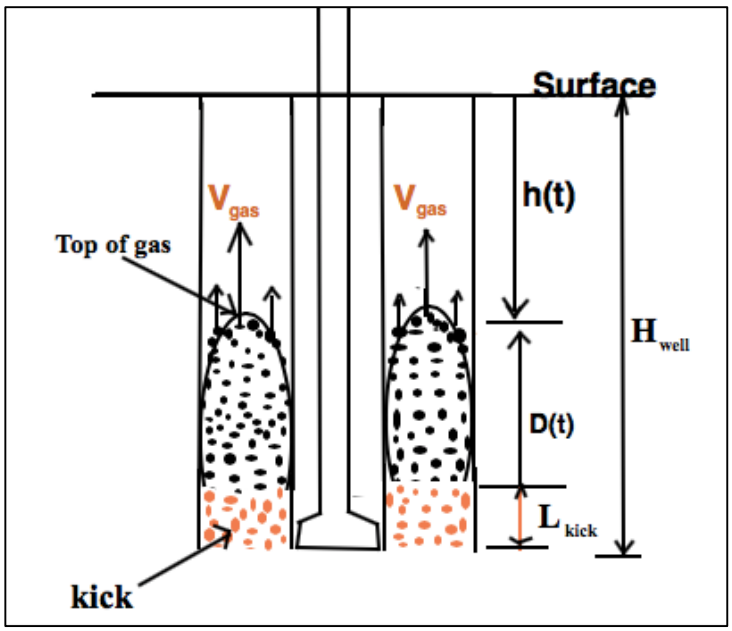

Figure 3-1: Gas rising up the annulus

Assuming that gas behaves as dispersed bubbles, the distance D(t) can expressed as:

$$D(t) = U_{gas}t \quad (3.2)$$

The depth h(t) from surface to the top of the gas column (mud-column overlying the gas column) can be estimated from the well depth minus the instantaneous distance covered by the gas column as:

$$h(t) = H_{well} - D(t) \quad (3.3)$$

Where H_{well} is the well depth and equation(3.3) can be used to calculate the hydrostatic pressure of the mud column overlying the gas column at any time t. This is just the mud weight multiplied with the depth h(t) and the gravitational constant. This is given as:

$$P(t) = \rho_{mud}\, g\, h_{mud}(t) \tag{3.4}$$

Where ρ_{mud} is the mud weight at the time kick is taken and $P(t)$ is the instantaneous hydrostatic pressure of the mud column overlying the gas column.

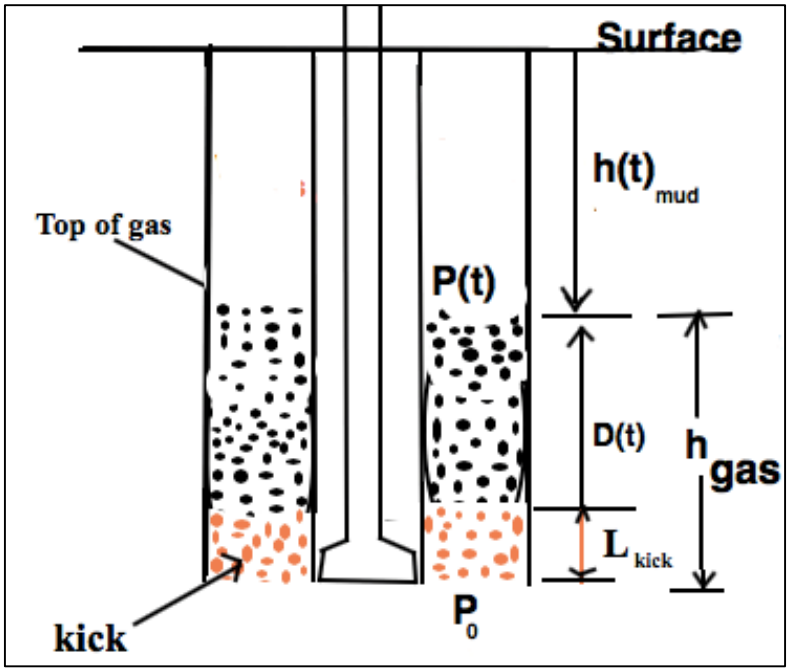

Figure 3-2: Determination of gas height in the annulus

As shown in Figure 3-2, gas height at time t is shown as $h_{gas}(t)$ and P(t) is the pressure at any time acting on top of the gas column. Using the ideal gas equation, the comparison between P(t) and P_0 can help to estimate the gas height, $h_{gas}(t)$. Assuming annular capacity is the same throughout the borehole, the relationship between $P(t)$ and P_0 is given as $P_0 L_{kick} = P(t)\, h_{gas}(t)$. Therefore, the height of the gas column as a function time t is given as:

$$h_{gas}(t) = \left(\frac{P_0}{P(t)}\right) L_{kick} \tag{3.5}$$

Where P_0 is the hydrostatic pressure of the original mud just before gas kick was taken and is given by $P_0 = \rho_{mud}\ H_{well}\ g$ and L_{kick} is the initial gas height at the time kick was taken.

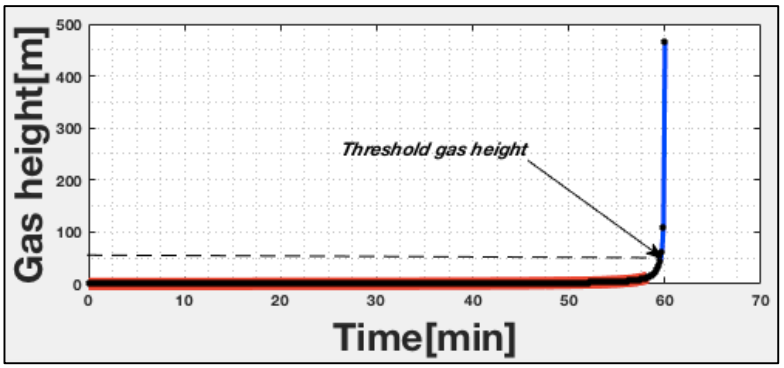

Figure 3-3: Gas expanding in the well

Figure 3-3 shows how gas expansion over time by simulating for gas height using equation(3.5). In this particular example, gas height was simulated by assuming a certain amount of gas enters inters the well due to underbalance and instantly after being detected, it gets circulated out while regaining control of the well. In this case, a gas influx flowing at the rate of $1.89m^3$/min(500gpm) into the well flowing at the rate of $3.4m^3$/min (900gpm). The kick is assumed to be taken at a depth 4000m and the gas and mud are assumed to form a two phase flow.

As shown in Figure 3-3, gas expansion takes place slowly until the gas expands enough to reach to a threshold amount. This threshold is the gas volume above which gas expands tremendously which may lead to more mud being displaced from the well. In this particular example, the threshold gas height was about 50m which took about 60minutes. At this height, the gas expanded two times to about 100m and finally to about 490m before the gas head reaches to the surface.

Due to gas expansion in the well as it is circulated out, the mud and gas columns keep changing with time. As the gas column increases due to expansion, the mud column above the gas column decreases correspondingly. This means that gas expansion displaces more mud in the annulus as gas is allowed to expand.

At this stage gas fraction can be deduced from the gas height given in equation(3.5) by estimating the volume of occupied by gas at time t and the volume of the mud in the well. This volume changes with time and is contributed by gas volume due to expansion $V_{expa}(t)$ and gas volume from

influx, $V_{inf}(t)$. The gas volume due to expansion is obtained by multiplying gas height given in equation(3.5) and the annular space(area) as $V_{expa}(t) = h_{gas}(t)\ A_{an}$ where A_{an} is the area of the annulus. The gas volume due to influx, $V_{inf}(t)$ is given by $V_{infl}(t) = q_{gas}\,t$ where t is the time taken after kick occurrence and this gives the gas volume at time t as:

$$V_{gas}(t) = V_{expa}(t) + V_{infl}(t) \tag{3.6}$$

Similarly, Volume of mud in the well is $V_{mud}(t) = h_{mud}(t)\ A_{an} + q_{mud}t$ where $h_{mud}(t)$ is the height occupied by the mud above the gas head as shown in Figure 3-2. The total volume in the annulus is given by the sum of mud volume and gas volume in the annulus at t. This is given as:

$$V_{total}(t) = V_{gas}(t) + V_{mud}(t) \tag{3.7}$$

The gas fraction is calculated using equation(2.7) as:

$$C_{gas}(t) = \frac{V_{gas}(t)}{V_{total}(t)} \tag{3.8}$$

3.2 Modelling Mud Weight as a Function of Time

In section 3.1 above, gas fraction as a function of time is derived and is given by equation(3.8). The expansion of the gas in the annulus causes the density of the mud – gas mixture becomes dependent on time as well. Combining equation(2.12) and (3.8) gives density of the mud - gas mixture as a function of time as:

$$\rho_{mix}(t) = \rho_{gas} C_{gas}(t) + (1 - C_{gas}(t))\,\rho_{mud} \tag{3.9}$$

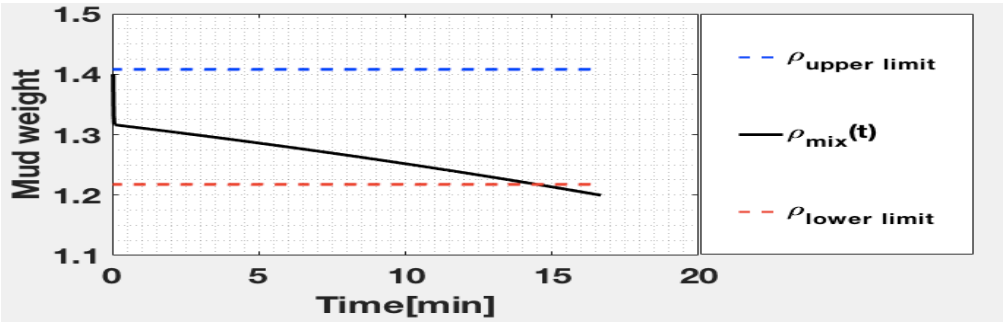

Figure 3-4: Mud weight as a function of time

Figure 3-4 shows how mud weight can change with time due to gas expansion in the well. The model given in equation(3.9) helps to estimate the density of the gas – mud mixture over time taking into account increase in volume due to expansion. This model reveals that mud weight drops abruptly at the start when the gas influx starts and takes a gradual decrease over time. This decrease may take a short interval of time to be noticed and normally setting upper and lower boundaries may help to identify the abnormality in the mud.

In Figure 3-4 the lower and upper boundaries are set to easily figure out how long mud weight drops to below the lower limit. A normal mud weight is the one in between the upper and lower boundaries and below or above it is said to be an abnormal mud weight. In this simulation, the mud weight dropped to below the lower limit just in about 15 minutes. This shows how rapidly the gas kick can be in affecting density and downhole pressure if not properly controlled.

4.0 Mud Weight as a Function of Pressure and Temperature

The presence of gas component in the mud makes the density of the cut mud, ρ_{mix} change with depth and time. The depth at which the gas kick is taken determines how much it can have impact on mud weight reduction and the longer the kick remains uncontrolled, the more the mud is cut. However, this is an indirect impact as the mostly affected parameter due to gas kick is the hydrostatic pressure which is a function of depth. Changing pressure and sometimes temperature in the bore hole changes the corresponding mud weight due to expansion of gas. Therefore, it is important to obtain the actual volume of the gas under changing conditions using the real gas law PV = ZnRT. With the gas volume, V_{gas1} at condition 1 known, the volume of the gas at condition 2 unknown, can be obtained using:

$$V_{gas2}(T_2, P_2) = V_{gas1}\left(\frac{Z_2 P_1 T_2}{Z_1 P_2 T_1}\right) \tag{4.1}$$

Where $V_{gas2}(T_2, P_2)$ is the volume of the gas at the new temperature and pressure conditions and T_2 and P_2 are the temperature and pressure respectively at the new conditions. The ratio of the volumes at the new conditions 2 to that at the previous conditions 1 gives the amount of how much gas expands between the two states. This factor is known as gas expansion factor K, and can be expressed as:

$$K = \frac{V_{gas2}}{V_{gas1}} = \left(\frac{Z_2 P_1 T_2}{Z_1 P_2 T_1}\right) \tag{4.2}$$

Similarly, the density of the gas at anew temperature and pressure condition, ρ_{gas2} with the density of gas at condition 1 known, ρ_{gas1} can be obtained using the law of conservation of mass. At the two conditions, mass of the gas in well remains constant meaning that only volume and density of the gas can change. Since density is inversely proportional to volume, equation(4.2) gives the relationship between densities at the two conditions of temperature and pressure as.

$$\rho_{gas2}(T_2, P_2) = K^{-1}\rho_{gas1} \tag{4.3}$$

Change in the volume of gas component due to change in temperature and pressure as given in equation(4.2) results into the change in volume of the mud – gas mixture. The new volume of the mud-gas mixture at new condition 2 can be expressed in terms of the new volume of the gas, V_{gas2} as:

$$V_{mix2}(T_2, P_2) = V_{mud1} + V_{gas2}(T_2, P_2) \tag{4.4}$$

Where $V_{mix2}(T_2, P_2)$ is the volume the mud – gas mixture at the new temperature and pressure conditions and V_{mud1} is the volume of liquid phase in the well. Since the volume of the liquid phase is given by $V_{mud1} = V_{mix1}\ (1 - C_{gas1})$ where V_{mix1} is the volume of the mud−gas mixture at condition 1. Substituting equation(4.2) and the definition of V_{mud1} into equation(4.4) and rearranging gives:

$$V_{mix2}(T_2, P_2) = V_{mix1}\left[(1 - C_{gas1}) + \left(\frac{Z_2 P_1 T_2}{Z_1 P_2 T_1}\right)\frac{V_{gas1}}{V_{mix1}}\right] \tag{4.5}$$

Since $\frac{V_{gas1}}{V_{mix1}} = C_{gas1}$, them substituting this definition into equation(4.5) gives:

$$V_{mix2}(T_2, P_2) = V_{mix1}\left[(1 - C_{gas1}) + KC_{gas1}\right] \tag{4.6}$$

Equation(4.6) can be used to estimate the new gas fraction C_{gas2} at the new temperature and pressure at conditions 2 using the definition of gas fraction given in equation(2.7) but in this case with $V_{gas} = V_{gas2}(T_2, P_2)$ and $V_{mix} = V_{mix2}(T_2, P_2)$ as $C_{gas2}(T_2, P_2) = \frac{V_{gas2}}{V_{mix2}}$. Combining these definitions and equation(4.6) gives:

$$C_{gas2}(T_2, P_2) = \frac{V_{gas1}\left(\frac{Z_2 P_1 T_2}{Z_1 P_2 T_1}\right)}{V_{mix1}\left[(1 - C_{gas1}) + \left(\frac{Z_2 P_1 T_2}{Z_1 P_2 T_1}\right)C_{gas1}\right]} = \frac{\left(\frac{Z_2 P_1 T_2}{Z_1 P_2 T_1}\right)\frac{V_{gas1}}{V_{mix1}}}{\left[(1 - C_{gas1}) + \left(\frac{Z_2 P_1 T_2}{Z_1 P_2 T_1}\right)C_{gas1}\right]} \tag{4.7}$$

Substituting $\frac{V_{gas1}}{V_{mix1}} = C_{gas1}$ in equation(4.7) and rearranging gives the final equation for gas fraction C_{gas2} at new temperature and pressure conditions 2.

$$C_{gas2}(T_2, P_2) = \left[1 + \left(\frac{1 - C_{gas1}}{C_{gas1}}\right)\left(\frac{1}{K}\right)\right]^{-1} \tag{4.8}$$

The mud cut density, $\rho_{mix2}(T_2, P_2)$ of the mud – gas mixture at new condition of temperature and pressure can be deduced using equation(4.8) and the law of conservation of mass. Since mud weight and volume do not change from one position to another, then using the law of conservation of mass, the mass of the mixture remains constant over all temperature and pressure ranges (i.e. $M_{mix1} = M_{mix2} = M_{mix}$). This allows re – definition of equation(4.6) in terms of density as $\frac{M_{mix}}{\rho_{mix2}(T,P)} = \frac{M_{mix}}{\rho_{mix1}}\left[(1 - C_{gas1}) + KC_{gas1}\right]$. Upon re – arrangement and simplification, the cut mud density at the new temperature and pressure condition is given as:

$$\rho_{mix2}(T_2, P_2) = \frac{\rho_{mix1}}{(1 - C_{gas1}) + KC_{gas1}} \tag{4.9}$$

Equation(4.9) shows that density of the cut mud changes with change in temperature and pressure caused by change in gas component which changes with changing temperature and pressure. It is indicated that the density varies directly proportional with pressure and inversely proportional with temperature.

5.0 Mud Weight as a function of Cuttings Concentration

Cuttings concentration leads to an increase in mud weight due to increased solids content in the mud. It is important to understand that drilled solids can sometimes compensate the effect of bottomhole pressure reduction in the wellbore caused by drilled gas(Goldsmith, 1972). This increase in bottomhole pressure is due to increase in mud weight.

5.1 Modelling Mud Weight as a Function of Cuttings

While drilling, cuttings are generated in the wellbore. The amount of cuttings depends on the rate of penetration, and can be expressed as:

$$q_{cuttings} = ROP.\frac{\pi. d_{bit}^2}{4} \tag{5.1}$$

Where ROP is the rate of penetration (m/hr) and d_{bit} is the bit diameter. The cuttings concentration at the bottom of the wellbore also known as original cuttings concentration, $C_{cuttings,\,o}$ is given as the function of the pump flow rate, q_{pump} and cuttings flow rate $q_{cuttings}$, Skalle (2015a).

$$C_{cuttings,o} = \frac{q_{cuttings}}{q_{cuttings}+q_{pump}} \approx \frac{q_{cuttings}}{q_{pump}} \tag{5.2}$$

Equation(5.2) gives the cuttings concentration at the bottom of the annulus. The density of the mud mixed with cuttings at the bottom of the annulus as a function of cuttings concentration is given as:

$$\rho_{mix} = \rho_{mud} + (\rho_{cuttings} - \rho_{mud}).\, C_{cuttings} \tag{5.3}$$

Equation(5.3) is valid only under assumptions that there is no gas or water influx in the well which would affect the density of the mixture.

5.2 Modelling Hydrostatic Pressure as a Function of Cuttings

The effect of cuttings concentration on bottomhole pressure can easily be investigated by using the relative hydrostatic pressure P_{rel}, of the mud column with and without cuttings into the mud assuming that the well is being drilled under the same speed such that density of the mud – cuttings mixture, ρ_{mix} remains constant. However, if the drilling rate is not constant, the density of the mud

– cuttings mixture might change correspondingly. The relative hydrostatic pressure may be given by:

$$P_{rel} = \frac{\rho_{mix}.g.TVD}{\rho_{mud}.g.TVD} = \frac{\rho_{mix}}{\rho_{mud}} = \frac{C_{cuttings}.\rho_{cuttings} + (1 - C_{cuttings})\rho_{mud}}{\rho_{mud}} \quad (5.4)$$

Re - arranging equation(5.4), an equation expressing relative hydrostatic pressure in the wellbore as a function of cuttings concentration is obtained.

$$Phyd_{rel} = \left(\frac{\rho_{cuttings}}{\rho_{mud}} - 1\right).C_{cuttings} + 1 \quad (5.5)$$

Equation(5.5) suggests that relative hydrostatic bottom hole pressure varies with change in cuttings concentration. Assuming that density of cuttings concentration is always greater than density of mud used, the increase in cuttings concentration will always result into a corresponding increase in hydrostatic pressure.

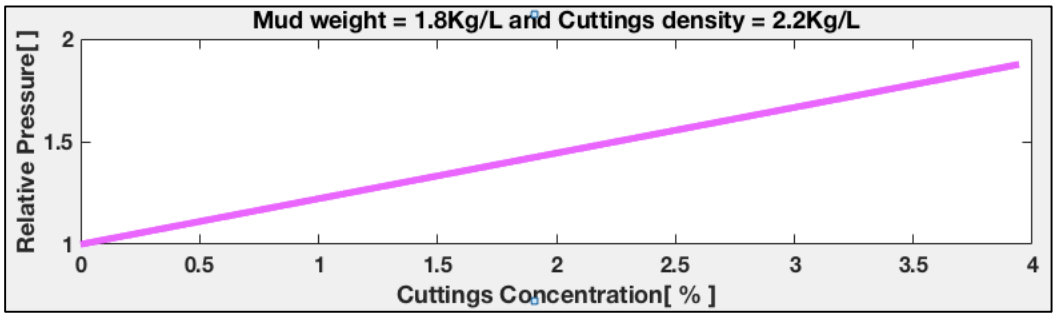

Figure 5-1: Relative Hydrostatic pressure under influence of cuttings

Figure 5-1 depicts the hydrostatic pressure variation due to change in cuttings concentration using equation(5.5). However, this observation could be opposite if the density of cuttings is less than that of mud used. Drilling through a formation whose cuttings density is less than that of the mud will relatively lower the hydrostatic pressure as cuttings concentration increases in the wellbore.

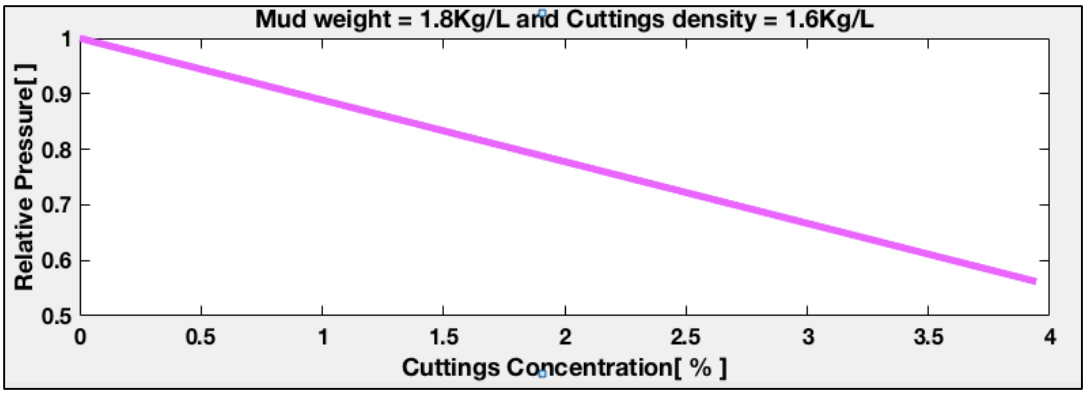

Figure 5-2: Relative Hydrostatic pressure under influence of cuttings

Figure 5-2 shows a negative impact of solids concentration in the wellbore on hydrostatic pressure when a formation of density less than that of drilling fluid is drilled through. This observation is known as solid cutting where increase in cuttings concentration leads to a corresponding decrease in the effective density of the mud – cuttings mixture. The two observations discussed can be used as important guides to the drilling crew in notifying them when the formation changes.

6.0 Modelling of Buoyancy Factor

Buoyancy factor is an important parameter to use in anticipating the real condition at the bottom of the well. It can be used to easily indicate changing conditions in the well especially change in mud weight. This goes in line with the ability of buoyancy factor to indicate changes in pressure which is obviously due to change in mud weight. This ability of buoyancy factor to indicate change in mud weight and pressure in the well can be used to predict the presence of a low density fluid(gas) in the well hence predicting the occurrence of gas kick due to its ability to change whenever mud weight and bottomhole pressure change.

In this thesis, buoyancy factor is modelled by using parameters that can affect it directly. These parameters include temperature, pressure, time and cuttings concentration. Buoyancy factor is modelled as a function of each parameter to indicate how they may affect change in buoyancy factor.

6.1 Buoyancy Factor as a Function of Gas Fraction

Buoyancy factor depends on mud weight of the drilling fluid in the wellbore. This is because change in mud weight leads to a significant change in buoyancy factor. The decrease in mud weight which is mainly due to influx of a formation fluid with lower density than the drilling fluid increases the buoyancy factor. A mathematical model for buoyancy factor which takes into account the variation of gas fraction in the mud mixture is established.

The buoyancy factor given in equation(2.4) can be expressed in terms of the gas fraction by substituting ρ_{mud} with the definition of ρ_{mix} . Combining equation(2.4) and equation gives:

$$\beta_{mix} = 1 - \frac{C_{gas} \cdot \rho_{gas} + (1 - C_{gas}) \cdot \rho_{mud}}{\rho_{steel}} \tag{6.1}$$

Rearranging equation(6.1) gives:

$$\beta_{mix} = 1 - \frac{\rho_{mud}}{\rho_{steel}} + \frac{C_{gas}(\rho_{mud} - \rho_{gas})}{\rho_{steel}} \tag{6.2}$$

Where C_{gas} is the average gas fraction in whole well and $\beta = 1 - \frac{\rho_{mud}}{\rho_{steel}}$ while $(\rho_{mud} - \rho_{gas}) = \Delta\rho_{mud}$. Where $\Delta\rho_{mud}$ is the change in density of the mud in the well.

Substituting the above definitions into equation(6.2) gives the final equation for buoyancy factor, β_{mix} of the mud – gas mixture in terms of the buoyancy factor of the uncut mud, β.

$$\beta_{mix} = \beta + \left(\frac{\Delta\rho_{mud}}{\rho_{steel}}\right). C_{gas} \tag{6.3}$$

Where $\Delta\rho_{mud}$ is the density difference between that of the original mud and density of the gas influx.

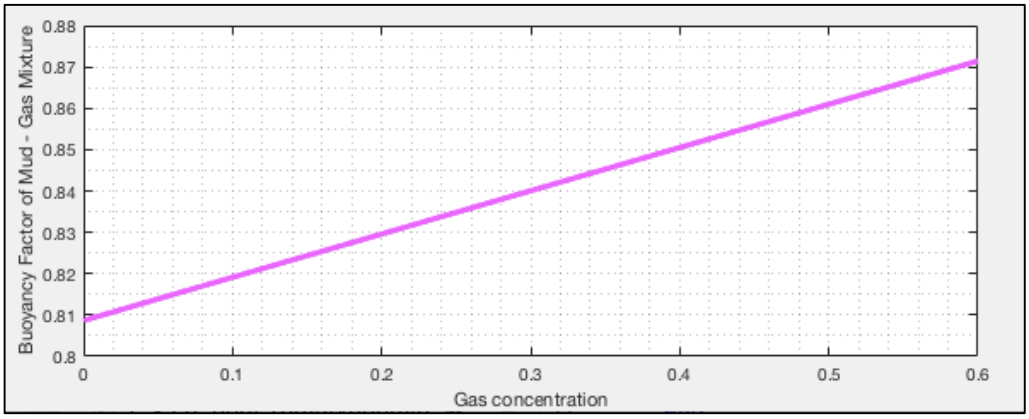

Figure 6-1: Relationship between buoyancy factor and gas fraction

Equation(6.3) suggests that buoyancy factor of the cut mud, β_{mix} is always greater than buoyancy of un cut mud β. This means that buoyancy factor increases as the gas fraction, C_{gas} increases. If the gas fraction is assumed to increases linearly, buoyancy factor increase linearly with gas fraction and this can be shown in Figure 6-1 which depicts how mud weight varies with the increase in the size of the gas influx. In this example, a mud weight equivalent to 1.5Kg/L was used as an initial mud weight.

6.2 Buoyancy Factor as a Function of Temperature and Pressure

Changing temperature and pressure have a direct impact on buoyancy factor especially when there is gas in the well. In section 4.0 above, effect of temperature and pressure on density of the mud was discussed revealing that temperature and pressure influences dramatic expansion of gas taken into the mud. Due to expansion of gas, a huge volume of mud can be displaced from the well leading to rapid decrease in bottom hole pressure.

The new buoyancy factor at the new temperature and pressure can be estimated by substituting equation(4.9) into equation(2.4) gives:

$$\beta_2(T,P) = \left(\frac{\rho_{mix2}(T,P)}{\rho_{steel}}\right) = 1 - \frac{\left(\frac{\rho_{mix1} Z_1 P_2 T_1}{Z_1 P_2 T_1 (1 - C_{gas1}) + Z_2 P_1 T_2 C_{gas1}}\right)}{\rho_{steel}} \quad (6.4)$$

Rearrangement gives the new buoyancy factor as:

$$\beta_2(T,P) = 1 - \left(\frac{\rho_{mix1}}{\rho_{steel}}\right)\left[\frac{1}{1 + (K-1)C_{gas1}}\right] \quad (6.5)$$

Where K = $\frac{Z_2 P_1 T_2}{Z_1 P_2 T_1}$ where K is the gas expansion factor. Equation(6.5) shows that gas expansion factor increases as gas expands. Since K is always greater than 1, then the ratio $\frac{1}{1 + (K-1)C_{gas1}}$ will be always less than 1. This means that there is a corresponding increase in buoyancy factor as the gas expands.

6.3 Buoyancy Factor as a Function of Time

The equation governing dependence of buoyancy factor on depth and time can be obtained by combining equation(2.4) and (3.9) of which upon simplification gives:

$$\beta_{mix}(t) = \beta_{OM} + \Delta\rho_{mud}\, C_{gas}(t) \quad (6.6)$$

Where $\beta_{OM} = 1 - \left(\frac{\rho_{mud}}{\rho_{steel}}\right)$ is the buoyancy factor of the original mud before the gas kick is taken and $\Delta\rho_{mud} = (\rho_{mud} - \rho_{gas})$. Equation(6.6) gives the buoyancy factor at a given depth and time. It shows that before the gas kick is taken, $\rho_{mud} = \rho_{gas}$ and this makes $\Delta\rho_{mud} = 0$, thus making the buoyancy factor equal to that of the original mud, β_{OM} as shown in Figure 6-2.

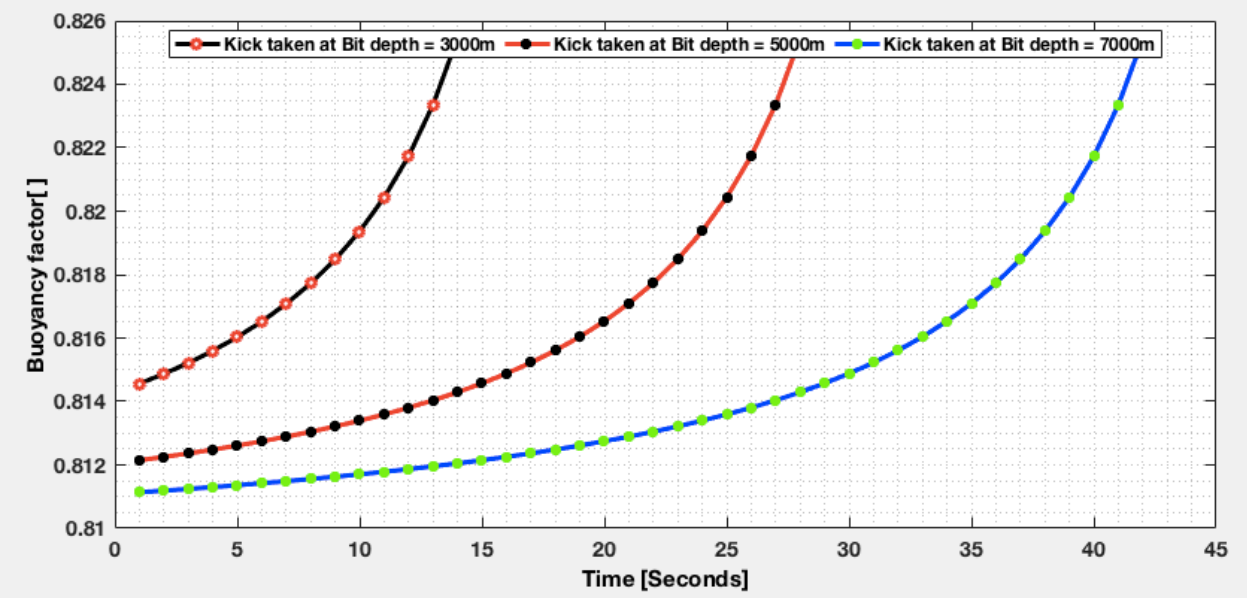

Figure 6-2: Buoyancy factor as a function of depth and time

Figure 6-2 shows simulation of a gas kick taken at different depths to anticipate the dependence of buoyancy factor on depth and time. The gas kick was assumed to be taken at a rate of 1.5m^3/sec and was circulated out using a mud weighted to 1.5kg/L flowing at a rate of 7m^3/sec. In this particular example, a gas kick was assumed to be circulated out at the instant it was taken. An assumption that gas expands as it is circulated out is also taken into account using the real gas behavior and finally it was assumed that the gas behaves as dispersed bubbles obeying equation(3.2).

The simulation shows that buoyancy factor is a function of both time and depth. In just 45 seconds, buoyancy factor changed from 0.81 to 0.83 as simulated in this example assuming that a gas kick of 1.5m^3/s was taken. This increase in buoyancy factor implies that mud weight has decreased correspondingly. Decrease in mud weight means that the ability of the mud to uplift the drill string decreases. Depending on the intensity of the gas kick taken, decrease in mud weight depends on time and depth as shown in Figure 6-2. However, the effect of gas expansion in the well bore on buoyancy factor remains fairly constant for some time before an abrupt increase happens. As shown in Figure 6-2 it took about 40 seconds before to reach to a significant increase in buoyancy

factor and after at about 45 seconds, buoyancy factor increased from 0.81 to about 0.83. This is an abrupt increase of about 0.2 in just 5 seconds.

This emphasizes that depending on the size of the gas kick taken and depth at which it is taken, a critical time and critical volume of gas have to be reached before a noticeable change in buoyancy factor happens. This critical volume is the minimum volume due to gas expansion above which buoyancy factor is noticeably changed due gas cutting while critical time is the minimum time taken from when gas enters the well bore to when a significant change in buoyancy factor is experienced.

6.4 Buoyancy Factor as a Function of Cuttings Concentration

In section 0 above, density of mud as a function of cuttings concentration was developed. In this section, buoyancy factor as a function of cuttings concentration is established. It is important to note that, normally density of cuttings is greater than density of the mud and cuttings grain density from different rock types ranges from 2.2 to 2.9kg/L, Bush & Freeman (1986). Combining equation(2.4) and equation(5.3) gives the buoyancy factor as:

$$\beta_{mix} = 1 - \frac{\rho_{mud} + (\rho_{cuttings} - \rho_{mud}).C_{cuttings}}{\rho_{steel}} \tag{6.7}$$

Rearranging equation(6.7) gives the final equation for β_{mix} as follows:

$$\beta_{mix} = 1 - \frac{\rho_{mud}}{\rho_{steel}} + \frac{C_{cuttings}\left(\rho_{mud} - \rho_{cuttings}\right)}{\rho_{steel}} \tag{6.8}$$

Substitution of $\beta_{OM} = 1 - \frac{\rho_{mud}}{\rho_{steel}}$ and $\Delta\rho_{mud} = \rho_{cuttings} - \rho_{mud}$ into equation(6.8) and rearranging gives:

$$\beta_{mix} = \beta_{OM} - \left(\frac{\Delta\rho_{mud}}{\rho_{steel}}\right). C_{cuttings} \tag{6.9}$$

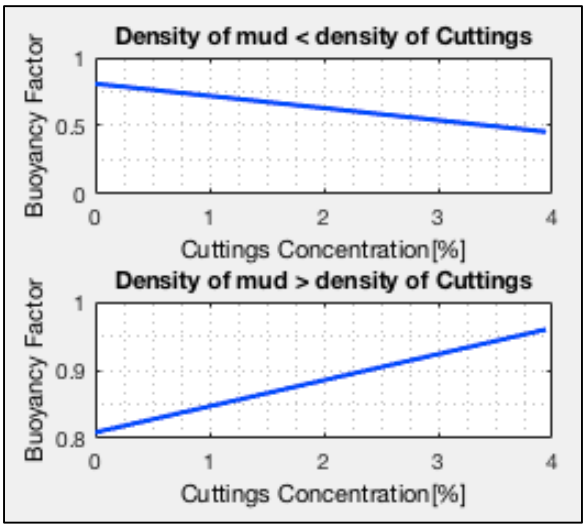

Figure 6-3: Effects of cuttings on buoyancy factor

Equation(6.9) suggests that buoyancy factor of the mixture of mud and cuttings varies linearly with cuttings concentration and that buoyancy decreases as cuttings in the mud increases provided that density of the mud is less than density of the cuttings. If lighter cuttings are drilled so that density of the mud is greater than density of the cuttings, buoyancy factor will increase instead of decreasing with cuttings concentration. The upper plot in Figure 6-3 shows the decrease in buoyancy factor taking into account that density of the mud is less than that of the cuttings while the lower plot shows that if density of the mud is greater than that of cuttings the buoyancy factor increases with cuttings concentration.

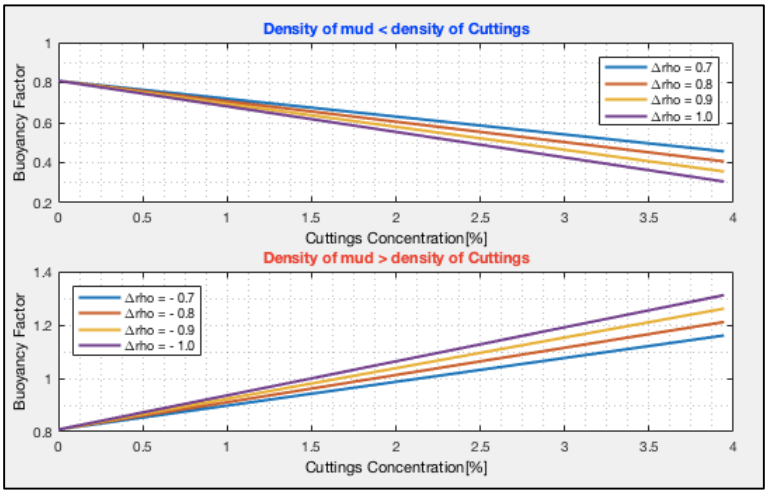

Figure 6-4: Effect of density differences on buoyancy factor

Increase in cuttings concentration is assumed to be the same in both cases and the only difference between the two cases is slope which determines whether the cuttings will have positive or negative effect on buoyancy factor. In Figure 6-4 the influence of the difference between density of the mud and that of cuttings is investigated to show how buoyancy factor varies with cuttings. In the upper plots, density of mud less than density of cuttings was used to calculate the buoyancy factor while in the lower plots density of mud higher than that of cuttings was used. As suggested in equation(6.9), the rate at which the buoyancy factor increases is proportional with the difference in the two densities or simply the slope. This effect is the same regardless of whether density of the mud is less or greater than density of cuttings.

Differentiating equation(6.9) with respect to cuttings concentration gives the change in buoyancy factor per unit increase in cuttings concentration as given in equation(6.10)

$$\frac{d\beta_{mix}}{dC_{cuttings}} = -\left(\frac{\Delta\rho_{mud}}{\rho_{steel}}\right) \tag{6.10}$$

Where$d\beta_{mix}$ is the change in buoyancy factor, $dC_{cuttings}$ is the change in cuttings concentration and $d\rho_{cuttings}$ is the change in cuttings density. Equation (6.10) suggests that change in buoyancy factor per unit change in cuttings concentration remains constant and is proportional with the difference between density of the mud and that of cuttings as shown in Figure 6-5. In both cases as indicated in upper and lower plots, change in buoyancy factor is higher for higher difference in mud weight.

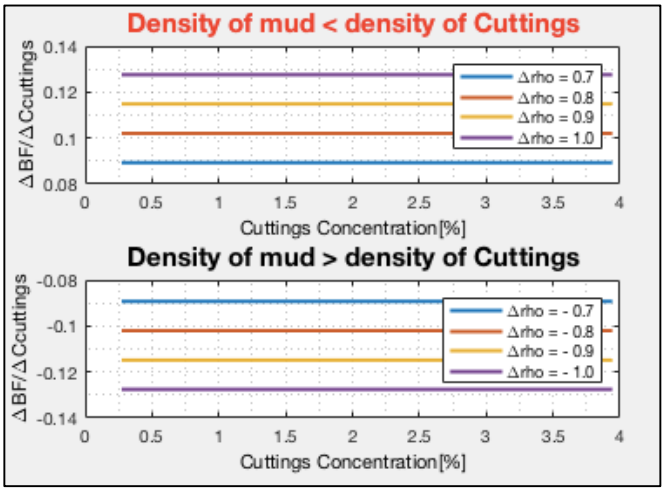

Figure 6-5: Influence of density differences on buoyancy factor

7.0 Bottomhole Pressure and Gas Fraction

Kick models to simulate for gas kicks into the well using downhole pressure and weight measurements need to be developed. Downhole pressure and weight gauges installed in the drill sting can be used to obtain the dynamic pressure and weight below it for components such as bottomhole assembly. In this thesis mathematical models for buoyancy factor are developed by converting the pressure and weight into buoyancy factor. To simulate the reality to the fullest is quite complicated and for that reason, in this section assumptions are included for well geometry by trying to make the model as simple as possible.

7.1 Variation in Bottomhole Pressure due to Gas Fraction

The serious consequence of formation gas flowing into the well is on bottomhole pressure reduction. This effect is due to the reason that gas expands rapidly and displaces large volume of mud from the well and due to its lowest density, the overall density of the gas is cut (reduced) which as a result decreases the hydrostatic bottomhole pressure.

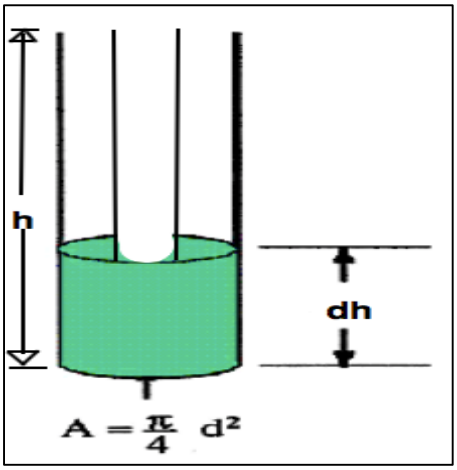

Figure 7-1: Pressure exerted by a small lamina

White, (1957) derived a modified equation for bottomhole pressure dependency on gas fraction following to the study done by Strong (1939) who established an equation known as Strong's equation which was erroneous. The derivation of the new equation was performed by considering pressure dP exerted by a small lamina dh at a depth h shown in Figure 7-1.

$$dP = \gamma(1 - C_{gas})dh \tag{7.1}$$

Where γ is the pressure per unit length and C_{gas} is the volume fraction of gas at depth h which can be expressed in terms of wellhead percent gas n, bottom and surface pressures, P_B and P_S respectively as:

$$C_{gas} = \frac{\left(\frac{nP_S}{P_B + P_S}\right)}{(100-n) + \left(\frac{nP_S}{P_B + P_S}\right)} \tag{7.2}$$

Combining equation(7.1) and equation(7.2) and rearranging gives:

$$dh = \frac{1}{\gamma}\left[dP + \frac{nP_S}{(100 - n)} \frac{dP}{(P_B + P_S)}\right] \tag{7.3}$$

Integration of equation over limits from P_B to P_S gives the hydrostatic head h:

$$h = \frac{1}{\gamma}\int_{P_B}^{P_S}\left(dP + \frac{nP_S}{100 - n}\frac{dP}{(P_B + P_S)}\right) = \frac{1}{\gamma}\left[P_B + \frac{nP_S}{(100-n)} \ln\left(1 + \frac{P_B}{P_S}\right)\right] \tag{7.4}$$

Reduction in bottomhole pressure can be obtained by rearranging equation(7.4) as:

$$\text{loss in head} = \Delta P_B = \gamma h - P_B = \frac{nP_S}{(100-n)}.2.03\log\left(1 + \frac{P_B}{P_S}\right) \tag{7.5}$$

Bottomhole pressure P_B can be solved numerically using equation(7.5). During a gas kick, the initial bottomhole pressure can be obtained using downhole pressure measurements and should be compared with the hydrostatic pressure γh before gas kick. If the two pressures are found to be different, γh can be used as the first approximation for bottomhole pressure in order to iteratively solve for bottomhole pressure. The process repeats over a number of iterations until convergence.

7.2 Simulation of Bottomhole Pressure

The algorithmic procedure for solving equation(7.5) is elaborated below where a step by step iterative procedure is established. In this iterative process to solve equation(7.5), assumption is made that the well is vertical and only influx is the only factor that leads to change in bottomhole pressure.

7.2.1 *Algorithmic Steps in simulating for bottomhole Pressure,* $\mathbf{P_B}$

Step 1: Initial value of bottomhole pressure P_B is calculated from true vertical depth h and specific density γ. This initial bottomhole pressure is given as $P_B^1 = \gamma h$

Step 2: Then the first value for loss in head is calculated as , $\Delta P_B^1 = \frac{nP_S}{100-n}.2.03\log\left(1+\frac{P_B^1}{P_S}\right)$ using the initial value of bottomhole pressure estimated in step 1 above.

Step 3: Using loss in head obtained in step 2, the new value for bottomhole pressure for second iteration can is calculated using the left hand-side of equation(7.5) as $P_B^2 = \gamma\, h\, - \Delta P_B^1$

Step 4: After obtaining the new value for bottomhole pressure, step 2 is repeated to obtain the new value for loss in head as $\Delta P_B^2 = \frac{nP_S}{100-n}.2.03\log\left(1+\frac{P_B^2}{P_S}\right)$. Step 2 through 3 are repeated up to convergence.

Equation(7.5) can be used to simulate the effect of gas kick on bottomhole pressure using algorithmic steps described above. Bottomhole pressure can be affected by a number of factors, other than gas at a time. Some of these are drill string rotation, cuttings concentration, swab and surge effects. In this thesis, only effect of gas in the wellbore is simulated for this particular example.

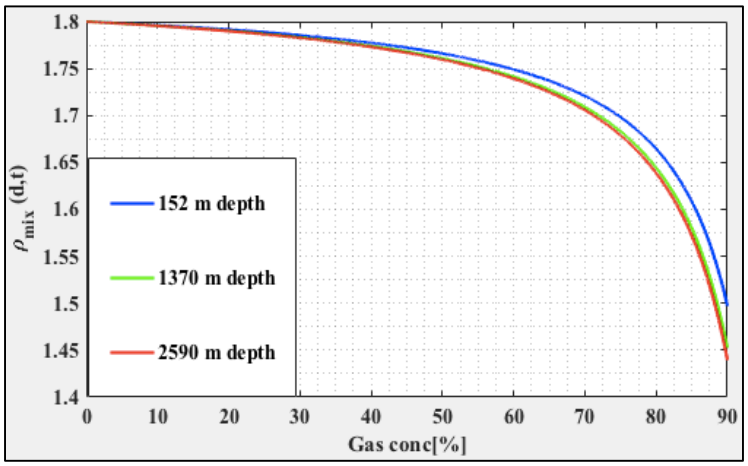

Figure 7-2: Apparent mud weight as a function of degree of gas fraction

The effect of gas in the mud for different depths was simulated. The result shows that mud weight decreases with increase in concentration of the gas. It is also observed from this simulation that

depth has influence on apparent mud weight and Figure 7-2 indicates that increase in the degree of gas present into the mud leads to decrease in apparent mud weight at the given depth. The deeper the kick is taken; the lesser effect it will have on apparent weight for the given concentration of gas.

Figure 7-3 shows how mud weight varies with depth. At about 60% fraction by gas, the apparent mud weight of 1.8kg/L is cut to about 1.6kg/L at the surface. It is also shown that the extent to which mud is cut at the surface depends on the degree of gas into the mud. The higher the degree of gas in the mud the higher the extent to which mud is cut at the surface.

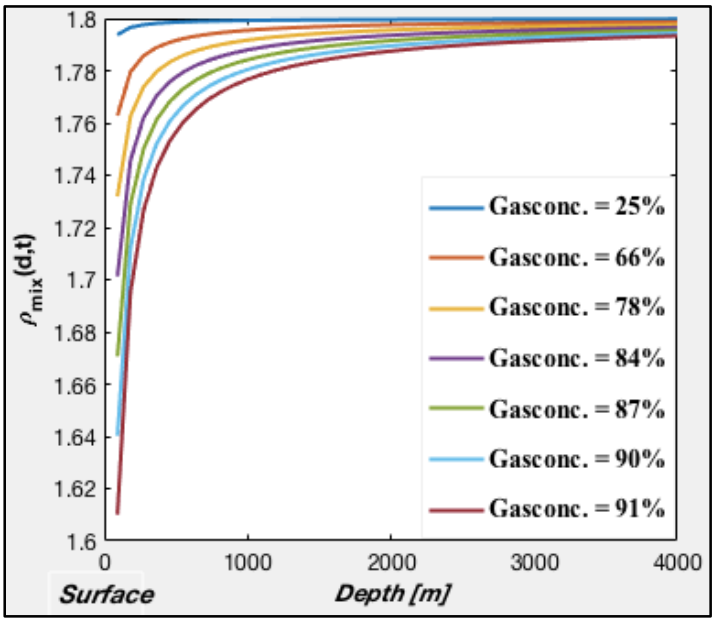

Figure 7-3: Mud weight as a function of depth and time

Apparent weight is also observed to be independent of depth for gas fraction low gas fraction. In Figure 7-3 the density of the mud – gas mixture remains fairly constant when simulated with a gas fraction of about 25%. This indicates that only in the presence of gas, mud at the surface can be reduced for a unit volume of gas taken at the bottom of the well. It is generally observed that at higher depths above 4000m, effect of gas into the mud weight is negligibly smaller and as it approaches at the surface, the effect is significantly high. This might be due to the reason that gas is compressed at higher depths and expands as it approaches at the surface where the hydrostatic pressure is low.

8.0 Modelling Buoyancy Factor for Vertical Well

Modelling buoyancy factor for a vertical well involves assumption that the wellbore is entirely vertical. Another assumption is that the drill string in the wellbore is concentric, although this assumption is not realistic because the drill string is normally erratic and has a tendency to wobble in the well. In reality the drill pipe can be positioned differently at different depths depending on hookload and hence touching the wall at some depths in the well(Wold & Kummen, 2015).

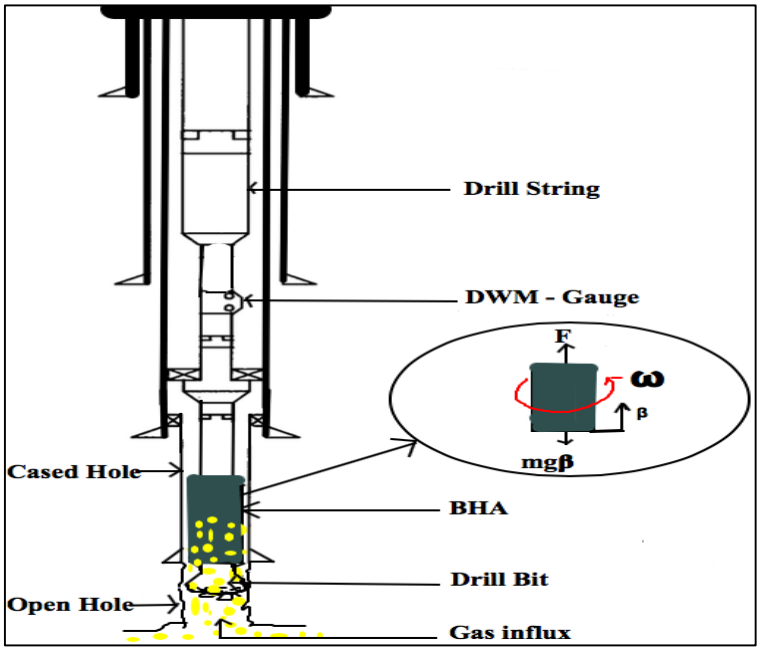

Figure 8-1: Vertical Wellbore Schematic

In the vertical well, friction force is assumed to be negligible due to rotation and wall contact forces (side forces) are regarded as negligible because the drill string does not touch the wall of the well. In the case of deviated well, effects of frictional forces, well geometry and side forces cannot be neglected and will be discussed in detail.

Figure 8-1 depicts the well in a vertical section with the drill bit off bottom and rotating with an angular speed ω. Gas kick is assumed to occur from the open hole section under the bit due to underbalance of bottom hole pressure caused by decrease in mud column in the annulus as the drill string is pulled up. The gas influx occurs at the bottom while the bit is off bottom and fills the area

around the BHA. Due to gas fraction in the annulus, the weight of the BHA changes with change in the size of gas influx. The weight of the BHA is measured by the Downhole Weight measurement(DWM) – gauge installed above it. This can be estimated mathematically by multiplying the weight of the BHA in air (i.e. mg) with the buoyancy factor β as $F = \beta W_{air}$. F is the apparent weight of the drill string element below the weight measurement gauge and W_{air} is its actual weight in air. The buoyancy factor β can be expressed as $\beta = \frac{F}{W_{air}}$ and since F is the apparent weight of the element below the weight measurement gauge, it can be obtained by taking the difference between the actual weight of the element W_{air} and the buoyant force F_b. Thus giving $F = W_{air} - F_b$ which gives the buoyancy factor as:

$$\beta = 1 - \frac{F_b}{W_{air}} \tag{8.1}$$

8.1 Buoyancy Factor of a Composite Drill String in a Vertical Well

Normally drill strings are composed of pipes with different sizes and properties. These may include drill pipes, heavy weight drill pipes and drill collars. Drill pipes have large internal diameters as compared to heavy weight drill pipes where by heavy weight drill pipes have small internal diameter thus making them heavier than drill pipes. Drill collars are characterized by high weight per unit length than heavy weight drill pipes. It is a usual practice to have drill collars just after the bit in order to provide the necessary weight on the bit. Heavy weight drill pipes follow after drill collars followed by drill pipes of the same or different diameters. Figure 8-2 shows an example of a composite drill string. Outer diameters of the drill string components increase as going from the top of the drill string down to the drill collar. This provides a surface area where the hydrostatic force due to drilling mud in the annulus acts. At each change in geometry, the hydrostatic force acts, whose magnitude is equal to the hydrostatic pressure times the projected area(Aadnoy et al, 1999).

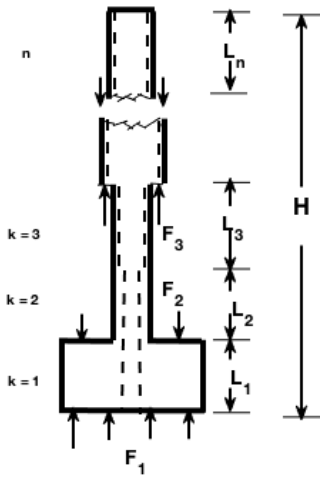

Figure 8-2: Composite drill string

Figure 8-2 is an example of a composite drill string with external forces acting on the drill string. The change in geometry provides forces on the drill pipes where by the buoyant force is then provided by the net force. The buoyant force at any depth can be obtained using the newton's second law(sum of F = 0) and this gives the buoyant force as $F_{bk} = \sum_{j=1}^{k} F_j$ starting from the bottom of the drill string. For instance, in Figure 8-2, F_1 and F_3 act vertically upwards while F_2 acts vertically downwards and hence opposes the two forces. The buoyant force is therefore given by the net force as $F_{b3} = F_1 + F_3 - F_2$.

These forces are obtained by multiplying the hydrostatic pressure at a given depth and the projected area at the point where there is change in geometry such as:

$$F_k = \begin{cases} \rho_m . g . \rho_k . H . A_k & \text{for } k = 1 \\ \rho_m . g . (H - D_k) A_k & \text{for } 2 \leq k \leq n \end{cases} \quad (8.2)$$

8.1.1 *Buoyancy Model by Piston Method*

Piston method also known as the force – area method is an approach that involves simple force balance. The buoyancy factor in this case can be obtained by balancing the buoyant force with the gravity weight of the drill string components at the point of interest. Taking the drill collar as an example, free body diagram is shown in Figure 8-3. The force balance gives the buoyed weight as

shown in Figure 8-3. The buoyed weight is then given by $W_{bouyed} = W_{dc} - F_{b1}$ which can also be expressed in terms of buoyancy factor as $\beta W_{dc} = W_{dc} - F_{b1}$. Then the buoyancy factor can be expressed as $\beta = 1 - \frac{F_b}{W_{dc}}$.

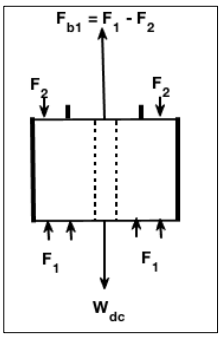

Figure 8-3: Free body diagram for the drill collar

Similarly, considering the whole drill string, the buoyancy factor can be give as the function of the buoyancy force F_{bk} at a given depth k as:

$$\beta_k = 1 - \frac{\sum_{j=1}^{k} F_j}{\sum_{k=1}^{n} w_k L_k} \tag{8.3}$$

Where w_k is the weight per unit length of the drill string component and L_k is its length. Equation (8.3) gives the local buoyancy factor. The overall buoyancy factor at the surface is given as:

$$\beta_k = 1 - \frac{\sum_{j=1}^{n} F_j}{\sum_{k=1}^{n} w_k L_k} \tag{8.4}$$

If the unit weight(s) of the drill string components are not specified, then w_k can be calculated using density of the material and its cross sectional area as $w_k = \rho_{steel}.\pi\left(R_k^2 - r_k^2\right)g$.

8.1.2 *Buoyancy Model by Law of Archimedes*

This method is widely used in the nearly all problems involving buoyancy for it gives the correct axial load. It is valid in many cases such as tubulars submerged in the drilling fluid and also is valid for both vertical and deviated wells. This method simply gives the buoyant force acting on a body as the force given by the weight of the displaced fluid(Aadnoy & Kaarstad, 2006; Aadnoy et al, 1999).

Equation(2.4) is the simplified model of the buoyancy factor of a submerged body. It is derived based on the Archimedes principle and can only be valid for a drill string submerged in the drilling fluid under the assumptions that the drill string is uniform and has the same internal and external diameters throughout the drill string. It also assumes that densities inside and outside the drill string are the same.

In some operations in the drilling process, densities inside the drill string may be different from that in the annulus. This may happen during cementing job where at first the inside mud is displaced by the cement slurry of heavier density than the mud in the annulus and lastly the cement in the drill string is displaced by the mud which is obviously lighter than the cement in the annulus.

During a kick, density of the mud in the annulus may become slightly different from that inside the drill string depending on the intensity of the kick. If too much volume of the influx is allowed to enter into the well, then the effect on the mud becomes tremendously high and the density of the mud – gas mixture becomes very low resulting into different densities inside and outside of the drill string.

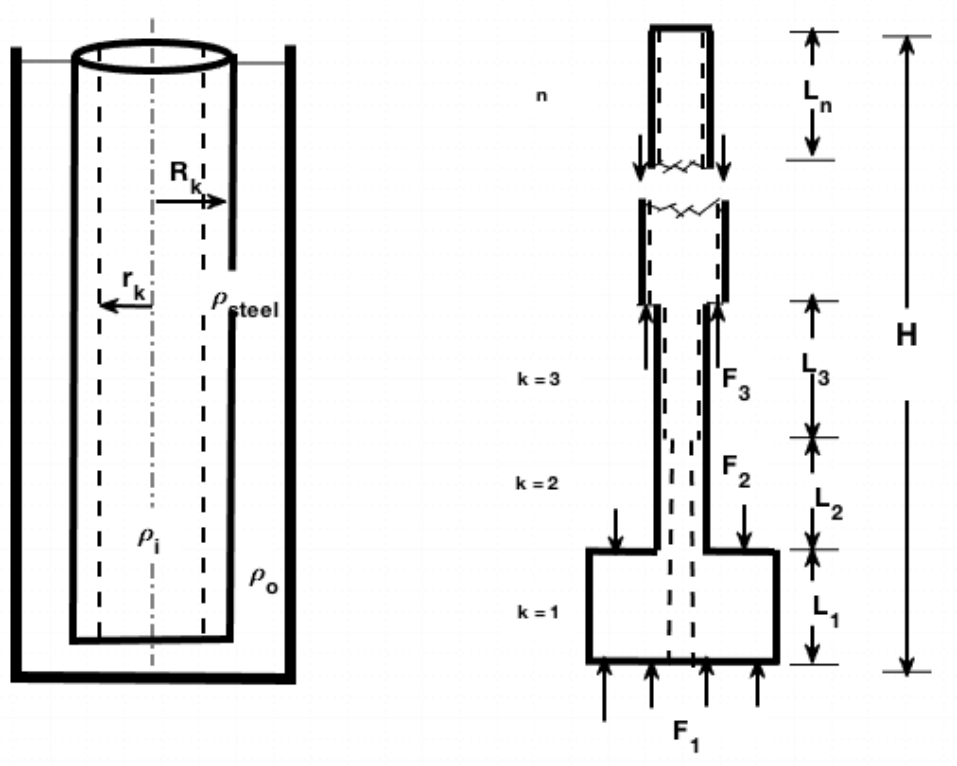

Figure 8-4: Different densities and different pipe sizes scenario

Considering the scenario shown in Figure 8-4 where the tubing is filled with mud of density ρ_i, and the outside annulus is filled with mud of density ρ_o. The bottom is assumed to sealed and according to Archimedes law, the weight of the pipe is assuming that is made of steel materials is given by $W = \rho_{steel}.V = \rho_{steel}\pi g\sum_{k=1}^{n}(R_k^2 - r_k^2)L_k$.The weight of the piper together with the mud inside is given by $W_{pm} = \rho_{steel}\pi g\sum_{k=1}^{n}\left[(R_k^2 - r_k^2)L_k + \rho_i\pi r_k^2 L_k\right]$.

The outside mud in the annulus provides the necessary buoyancy for the total volume of drill string plus the mud inside. The weight of the displaced mud in the annulus is given as the function of outside mud density is $W_{dm} = \rho_o\pi g\sum_{k}^{n} R_k^2 L_k$. The buoyed weight is equal to difference between the weight of the drill string plus the mud inside W_{pm}, and the weight of the mud displaced W_{dm} as $W_{buoyed} = W_{pm} - W_{dm} = \rho_{steel}\pi g\sum_{k=1}^{n}\left[(R_k^2 - r_k^2)L_k + \rho_i\pi r_k^2 L_k\right] - \rho_o\pi g\sum_{k}^{n} R_k^2 L_k$. The buoyancy factor is equal to the ratio between the buoyed weight and the weight of the drill string given by $\beta_k = \frac{W_{buoyed}}{W} = \frac{\rho_{steel}\pi g\sum_{k=1}^{n}\left[(R_k^2 - r_k^2)L_k + \rho_i\pi r_k^2 L_k\right] - \rho_o\pi g\sum_{k}^{n} R_k^2 L_k}{\rho_{steel}\pi g\sum_{k=1}^{n}(R_k^2 - r_k^2)L_k}$. Simplifications gives the effective buoyancy factor at any depth as given in equation(9.4) as:

$$\beta_k = 1 - \frac{\sum_{k=1}^{n}(\rho_o R_k^2 - \rho_i r_k^2)L_k}{\rho_{steel}\sum_{k=1}^{n}(R_k^2 - r_k^2)L_k} \tag{8.5}$$

Equation (8.5) gives the local buoyancy factor at the given depth. It is obvious that Equation(9.4) is the detailed version of equation(2.4) and for equal fluid densities inside and outside the drill string, equation(8.5) is reduced to the simplest form of buoyancy factor in equation(2.4).

8.1.3 *The Piston Buoyancy Model vs. Archimedes Buoyancy Model.*

As stated earlier that the two buoyancy models give the same axial weight at the surface. However, the local buoyancy factors at a particular depth might be different and hence giving different axial weights a given depth. To figure out how these models can approximate the buoyancy factors as well as the axial weights, data from the work by Aadnoy & Kaarstad (2006) was used. In this work, the overall buoyancy factors for a tapered string were calculated using the Archimedes approach. Data used for the calculations are shown in Table 8-1.

Table 8-1: Data for tapered drill string(Aadnoy & Kaarstad, 2006)

Pipe:	Depth mTVD	Size[in]	Weight [kN/]	Buoyancy factor, β
Drill pipe −1	1000	$6\,5/6$ x 5	0.73	β_4
Drill pipe −2	1500	5 x 4	0.294	β_3
HWDP	1800	5 x 3	0.62	β_2
Drill collars	1900	8 x 3	2.13	β_1

In this thesis, the buoyancy factors and axial weights are calculated using the Archimedes buoyancy model and the piston buoyancy model. In addition, the different density scenario was used where the density of the mud inside the drill string was 1.8kg/L while that of the mud outside the drill string was 1.4kg/L and the density of steel used was 7.8kg/L The results from the two models are presented in Table 8-2

Table 8-2: Results from Archimedes and Piston Buoyancy Models

Pipe:	Depth mTVD	Buoyancy factor, β		Axil Load	
		Archimedes Model	Piston Model	Archimedes Model	Piston Model
Drill pipe −1	1000	0.88	0.69	1118	1114
Drill pipe −2	1500	0.86	0.78	470	505
HWDP	1800	0.84	0.78	335	335
Drill collars	1900	0.83	0.47	177	104

As shown in Table 8-2 buoyancy factors at a given depth are different for the two methods. This difference is also seen for the case of buoyancy factors. However, the two methods provide the same axial weight(Hookload) of the drill string at the surface.

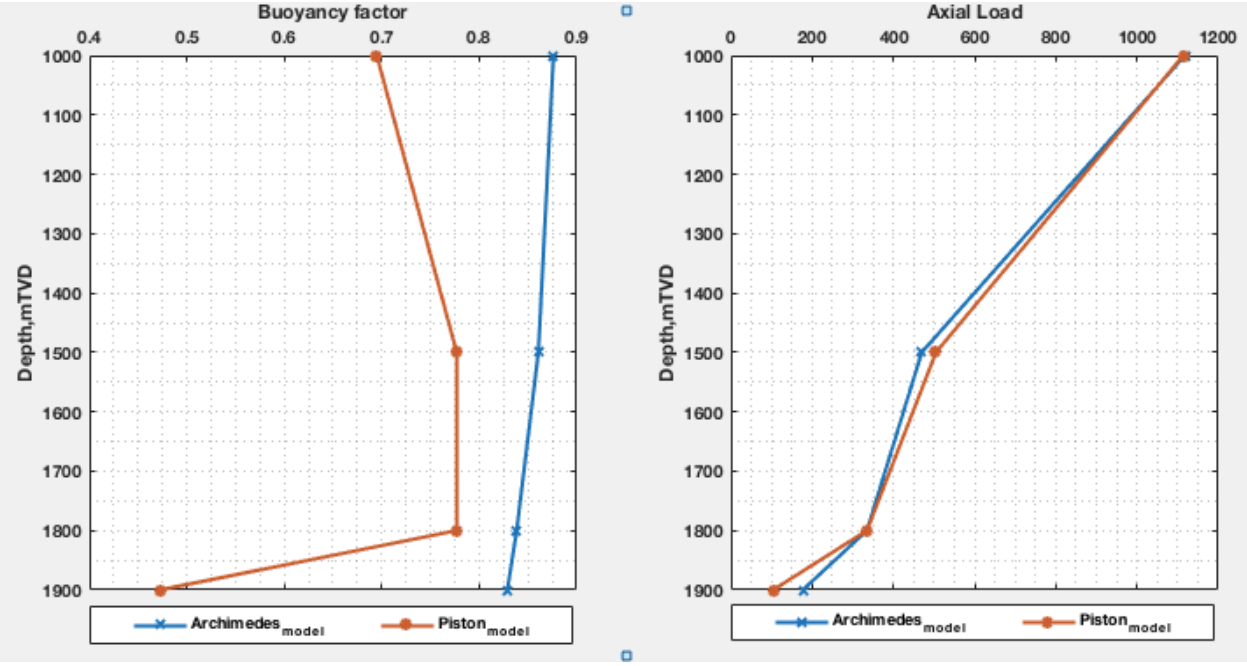

Figure 8-5: Archimedes and Piston models compared

Figure 8-5 shows the comparison between the Archimedes and piston models for buoyancy factor and axial loads on the drill string. There are slight differences on the results obtained from the two models but as shown in the figure, the two methods give approximately the same axial load at the surface. However, the Archimedes model gives the most correct result than the piston model and can be used to solve nearly all problems involving buoyancy(Aadnoy et al, 1999).

9.0 Modelling Buoyancy Factor for a Deviated Well

Buoyant force on a drill string in a vertical well acts at the bottom end of the drill pipe because only the bottom is in contact with upward force exerted by the fluid. This is different for a deviated wellbore where the buoyant force in this case is distributed along the pipe The buoyancy factor acting along the drill string in a vertical section is therefore assumed to be equal to one except at the bottom most part of the drill string and is less than one for a deviated wellbore section. Modelling of buoyancy in a deviated well needs taking into account that buoyancy factor will be distributed alongside the well bore.

However, it is somewhat unrealistic to have a mathematical model for buoyancy factor for the whole drill string in the deviated well due to the fact that geometry can have a big influence in changing the buoyancy factor between two successive points in the well. It is therefore important to have a mathematical model which evaluates buoyancy factor by considering small drill string elements so that it makes easy to account for a geometrical effect on each element rather than the whole drill string at once. In this section, buoyancy factor for a deviated borehole is derived by taking into account change in the inclination angle.

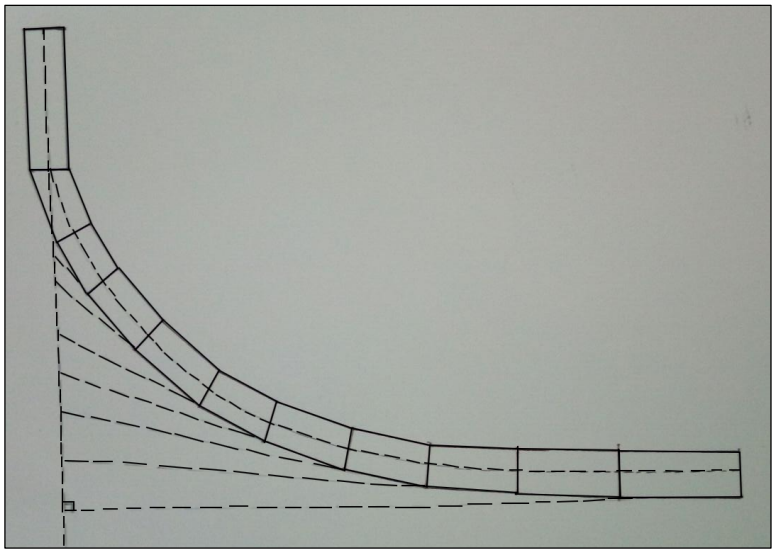

Figure 9-1: Schematic view of a deviated borehole

The schematic well in Figure 9-1 shows that as the well path deviates from vertical, the angle of inclination changes at an equivalent rate equal to the walk rate. The inclination starts at 0^0 where

the wellbore is said to be in a vertical section to 90^0 where the wellbore is said to be in a horizontal section. As indicated in Figure 9-1, the inclination angle at an point on the drill pipe is defined by the tangent line to that point. It is clearly shown that the angle of inclination is never constant between two points in the deviated borehole and increases as the well path changes from vertical to horizontal. This goes in line with buoyancy factor that as angle of inclination changes between two points, then the buoyant forces at the two points will be different as well.

It is intuitively known that buoyancy factor takes care of the weight of the fluid that a particular body is capable of displacing when submerged into that fluid. This means that, for a drill string submerged in the deviated borehole, the buoyant force will also change for each unit length of the drill string element due to change in the surface area in contact with the drilling fluid. This surface area is the projected area of the drill string which acts perpendicular to the buoyant force as shown in Figure 9-2

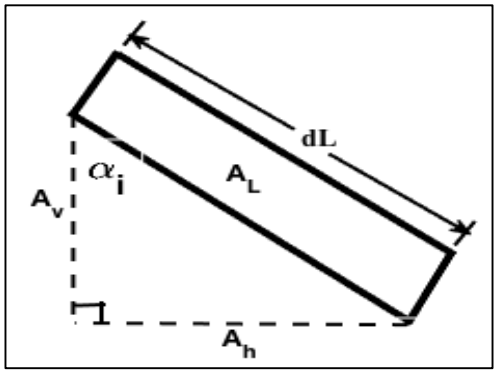

Figure 9-2: Weight of the drill pipe in a deviated borehole

Figure 9-2 shows a drill pipe resting on the low side in a deviated borehole at an inclination angle α_i. The surface area of drill pipe in contact with drilling fluid is decomposed into vertical and horizontal components. These components are given are $A_h = A_L \sin\alpha_i$ and $A_v = A_L \cos\alpha_i$ respectively. A_L is the lateral surface area of the cylindrical drill pipe of length dL_i and is given as $A_L = 2\pi r dL_i$. The projected surface areas become $A_h = 2\pi r dL_i \sin\alpha_i$ and $A_v = 2\pi r dL_i \cos\alpha_i$.

The drill pipe submerged in the drilling fluid is acted upon by gravity weight W of the drill pipe, buoyant force F_b, Wall force W_n and axial force W_a as shown in Figure 9-3. The buoyant force and gravity weight act vertically upwards and downwards respectively. The wall and axial forces are

components of the net gravity weight also known as the buoyed weight W_b, and the wall force acts perpendicular to the surface of the drill pipe while the axial force acts parallel to the surface of the drill pipe. The buoyed weight of the drill pipe is given by $W_b = \beta W$, where β is the buoyancy factor. The wall force and axial weight are given by $W_n = W\sin\alpha_i$ and $W_a = W\cos\alpha_i$ when the drill pipe is in air and when submerged in the drill fluid $W_n = \beta W\sin\alpha_i$ and $W_a = \beta W\cos\alpha_i$. The orientation and direction of all forces acting on the drill pipe are presented in the force diagram as shown in Figure 9-3

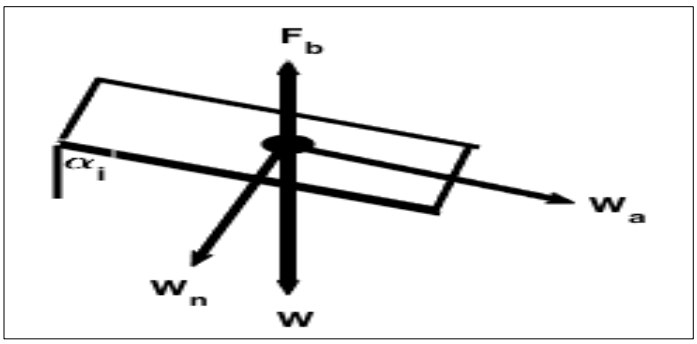

Figure 9-3: Forces acting on a drill pipe submerged in the drilling fluid

The wall force and axial forces are very important in evaluating the tension or compression forces acting on the drill string. The tension force F is given as the function of buoyancy factor and coefficient of friction between the wall of the well and surface of the drill pipes. This is given by $F = W_a \pm \mu W_n$ where $+$ is for pulling out of the hole and $-$ is for running into the hole. Substituting the definitions of W_a and W_n equation(9.1) is obtained, (Aadnoy & Djurhuus, 2008); Aadnoy & Huusgaard (2002)

$$F = \beta W(\cos\alpha_i \pm \mu \sin\alpha_i) \tag{9.1}$$

As stated earlier, the buoyant force F_b acts vertically upwards and opposite to the gravity weight W. This buoyant force is provided by the hydrostatic pressure difference acting at the lower and upper sides of the drill pipe. It has been pointed out that, when the drill pipe is submerged into the deviated borehole, the buoyant force will be distributed along the entire drill pipe. This buoyant force acts vertically upwards along the drill pipe.

Figure 9-4 depicts a small element of the drill pipe being acted upon by two forces F_1 and F_2 in a curved section where F_1 acts downwards and F_2 acts upwards. The two forces are equal to the hydrostatic pressures times the perpendicular surface area of the pipe element and are given by $F_1 = P_1\ A_h$ and $F_2 = P_2\ A_h$. The hydrostatic pressures are given by $P_1 = \rho_{mud}.g.TVD_1\ A_h$ and $P_2 = \rho_{mud}.g.TVD_2\ A_h$. Then substation of these definitions gives the downward and upward forces as $F_1 = \rho_{mud}.g.TVD_1\ A_h$ and $F_2 = \rho_{mud}.g.TVD_2\ A_h$. The two forces are not equal as they act different depths with F_2 being greater than F_1.

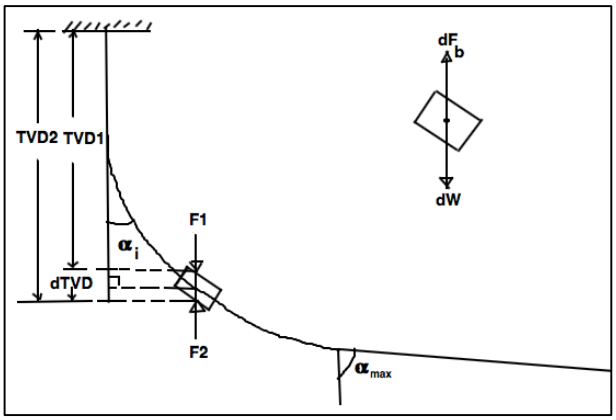

Figure 9-4: Buoyant force due to pressure differences

The difference between these forces provides the buoyant force dF_b which is the net upward force. This force is given by $dF_b = F_2 - F_1$ and substitution gives $dF_b = \rho_{mud}.g.(TVD_2 - TVD_1)A_{eff}$. Where A_{eff} is the effective surface area in contact with each force. This is equal to half of the projected lateral surface area and is given by $A_{eff} = \frac{1}{2}A_h$. It has been stated earlier that A_h is the projected area of the lateral surface area of the small element and is given by $A_h = 2\pi r_i dL_i \sin\alpha_i$. Therefore, the effective surface area on which each force acts is $A_{eff} = \pi r_i dL_i \sin\alpha_i$. Substituting these definitions we get the buoyant force as $dF_b = \pi r dL_i.\rho_{mud}.g.(TVD_2 - TVD_1)$ and finally substituting $TVD_2 - TVD_1 = \Delta TVD_i$ gives the buoyant force as:

$$dF_b = \pi r_i dL_i.\rho_{mud}.g.\Delta TVD_i.\sin\alpha_i \qquad (9.2)$$

The change in TVD, ΔTVD_i in equation(9.2) can be simply calculated by decomposing the length of the element simply into the vertical component as $\Delta TVD_i = dL_i \cos\alpha_i$. However, this can be

applied only to the sections like in the tangent section where the angle of inclination remains fairly constant over the entire section. For the case of the curved section, survey calculation methods should be used. These methods include the tangential method, balanced tangential method, average angle method, radius of curvature method and the minimum curvature method. Among these, the minimum curvature method is said to be the most accurate method of estimating the well bore trajectory and the tangential method being the most erroneous(Farah, 2013). In this thesis, the minimum curvature method will be discussed and used for sample calculations in estimating the change in vertical depth, ΔTVD_i.

9.1 ΔTVD for Curved Section by Minimum Curvature Method

Minimum curvature method is the modification of the balanced tangential method which takes the space vectors defined by inclination and direction measurements and smooths them onto the wellbore curve, Farah (2013). The main difference between minimum curvature method and the tangential method is that minimum curvature method replaces straight lines with the circular arc. Thus instead of using straight lines to approximate the wellbore path, minimum curvature method uses an arc which is calculated by using the dogleg factor using the amount of angular change over the course length, Farah (2013)

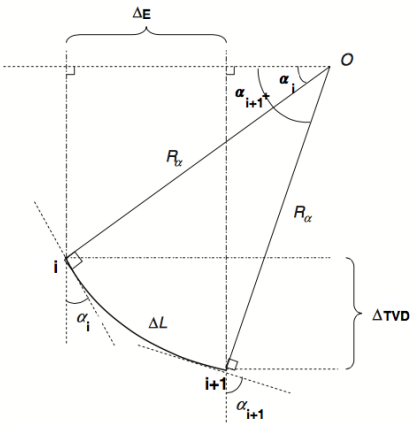

Figure 9-5: Projection of a wellbore in a vertical plane

As shown in Figure 9-5 the well path is estimated approximated by the circular arc using a ratio factor RF. This ratio factor is calculated from the dogleg angle. The dogleg angle ϕ is calculated

from the inclination angles and azimuth and from two successive survey points on the curve and is given by $\phi_i = \cos^{-1}[\cos\alpha_i \cos\alpha_{i+1} + \sin\alpha_i \sin\alpha_{i+1} \cos(\beta_{i+1} - \beta_i)]$ where α_i and α_{i+1} are inclination angles at the two successive survey points i and i+1 on the curve while β_i and β_{i+1} are the azimuth angles at the two survey points respectively. Then the ratio factor can be calculated by using the dogleg angle and is given by $RF_i = \frac{2}{\phi_i}\left(\frac{180}{\pi}\right)\tan\frac{\phi_i}{}$. Having obtained the ratio factor RF, the change in vertical depth ΔTVD_i, change in easting ΔTVD_i and change in northing ΔTVD_i, can be calculated using equation(9.3).

$$\Delta TVD_i = \frac{\Delta L}{2}.RF_i(\cos\alpha_i + \cos\alpha_{i+1})$$
$$\Delta E_i = \frac{\Delta L}{2}.RF_i(\sin\alpha_i \sin\beta_i + \sin\alpha_{i+1} \sin\beta_{i+1}) \quad (9.3)$$
$$\Delta N_i = \frac{\Delta L}{2}.RF_i(\sin\alpha_i \cos\beta_i + \sin\alpha_{i+1} \cos\beta_{i+1})$$

ΔL in equation(9.3) is the change in measured depths between the two survey points. This needs to be as small as possible so as to increase accuracy.

9.2 Wellbore Profile for Well AA

Equation(9.3) was applied on the well path data provided in Table 9-1. These data were used in the work published by Aadnoy & Kaarstad (2006). The name "Well AA" is an abstract name given to the well data which were provided in this work.

Table 9-1: Well path data for deviated well(Aadnoy & Kaarstad, 2006)

Position	Depth mTVD	Depth mMD	Inclination(°)	Radius(m)
Kick-off depth	1000	1000	0	–
End of build up	1433	1524	0 – 60	500
Top drill collars	2000	2658	60	–
Drill bit	2100	2858	60	–

The aim for this sample calculation is to test and validate the well profile model given in equation(9.3) in order to be sure that the when determining the buoyancy factor for each drill string element in a deviated well, the well profile is accurately estimated to avoid possible errors due to wrong geometrical approximations. Table 9-1 presents the well data which were used for this well and were compared with the results obtained from the minimum curvature model. The results from calculations are shown in Table 9-2. The well curvature was dived into N number of segments with a segment length of 1meter of measured depth. The inclination angle was determined by dividing the angle in the curved section with a small increment of 0.1145° per each meter increase in measured depth.

Table 9-2: Results from minimum curvature model

Position	Depth mTVD (Given)	Depth mTVD (Calculated)	Deviation (m)
Kick-off depth	1000	1000	0
End of build up	1433	1433.3	0.3
Top drill collars	2000	2000.3	0.3
Drill bit	2100	2100.3	0.3

The results from minimum curvature method show very small deviations from the actual values. Comparison is done on the true vertical depths because it is the very sensitive parameter when calculating the buoyancy factor on the drill string in a deviated well. The well profile for the given data provided in Table 9-1 are presented in Figure 9-6 using the calculated data. The upper plot is a two dimensional profile showing the true vertical depth versus the horizontal departure. This is typically the J – well for a deviated borehole. The lower plot is the three – dimensional profile of the J – well. These profiles indicate that the minimum curvature model provided in equation(9.3) approximates the true well profile of the deviated well. This turns out that this model can be used to calculate for the true vertical distances and especially change in the true vertical distances which can be used to calculate the buoyancy factor as a function of borehole geometry. Having estimated

change in true vertical distances ΔTVD_i, then the buoyant model given in equation(9.2) which is a function of ΔTVD_i can be obtained.

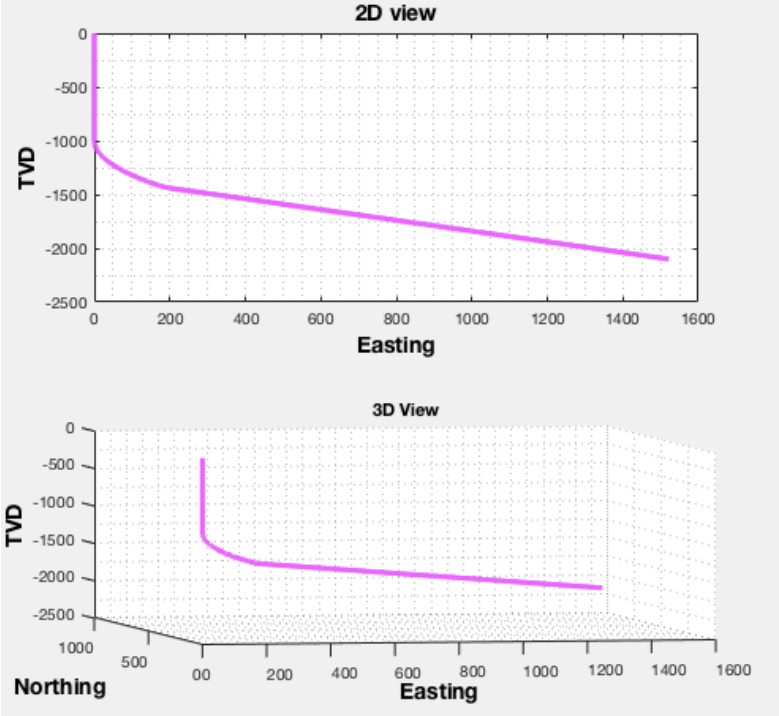

Figure 9-6: Wellbore profiles

This buoyancy model will take into account the well geometry by dividing the drill string into small elements. Buoyancy model will be used to estimate the buoyancy on each element as a function of change in vertical depth.

9.3 Buoyancy Model for Deviated Wellbore

The buoyancy model for a deviated borehole is derived by taking into account change in geometry of the borehole which leads to changes in inclination angle. It is a real assumption that for a fluid to have effect on weight of the body submerged into it, there must be surface area on which the fluid act. Since this surface area in contact with the drilling fluid must vary as the wellbore geometry changes. The effect of change in geometry on buoyancy factor may be more pronounced in a curved and inclined sections while in the vertical section the buoyancy factor is equal to 1 and

remains unchanged for the entire vertical section(Hovda, 2017). The biggest challenge is to know how buoyancy factor changes as the inclination angle starts to increase from zero.

To anticipate this, the buoyancy model is developed by balancing the buoyant force given by equation(9.2) and the gravity weight. The free body diagram in shows the two forces acting opposite to each other. The net force between the two forces gives the buoyed weight dW_{buoyed} , of the small element submerged in the drilling fluid in a deviated borehole. This buoyed weight is given by $dW_{buoyed} = dW - dF_b$.

The buoyed weight can be calculated as the product of the gravity weight and the buoyancy factor β as $dW_{buoyed} = \beta\, dW$. Upon substitution and simplification, the buoyancy factor can be given by $\beta = 1 - \frac{dF_b}{dW}$. The gravity weight dW is given by wdL_i where *w* is the unit weight of the drill string element i and dL_i is its length. The unit weight *w* is given in terms of density of the material of the drill string element as $w = \rho_{steel}.g.A_i$ where A_i is the cross sectional area of the drill string element given as $A = \pi r_i^2$ where r_i is its radius. Substitution of these definitions gives the buoyancy factor as:

$$\beta_i = 1 - \frac{dF_b}{\rho_{steel}.g.\pi r_i^2.dL_i} \tag{9.4}$$

Equation(9.4) gives buoyancy factor as a function of buoyant force acting on a small element of length dL. Substituting equation(9.2) into equation(9.4) gives $\beta_i = 1 - \frac{\pi r_i.dL_i.\rho_{mud}.g.\Delta TVD_i.\sin\alpha_i}{\rho_{steel}.g.r_i^2.dL_i}$. Simplification and re – rearrangement gives the final model for the buoyancy factor on a drill string element i as:

$$\beta_i = 1 - \left(\frac{\rho_{mud}}{\rho_{steel}}\right)\left(\frac{\Delta TVD_i}{r_i^2}\right)\sin\alpha_i \tag{9.5}$$

Equation(9.5) is the buoyancy model for a deviated borehole which takes into account the geometrical parameters of the well path and drill pipe sizes. The buoyancy factor changes with change in inclination angle α_i and for every change in true vertical depth ΔTVD_i. Equation (9.5) was applied to the well data provided in Table 9-1 in order to simulate and figure out how the buoyancy factor changes with inclination especially in the curved section. The well path was divided into small section lengths dL_i which was then converted into their corresponding change

in true vertical depth ΔTVD_i using the minimum curvature model given in equation(9.3). The resulting buoyancy factor calculated using equation (9.5) is shown in Figure 9-7.

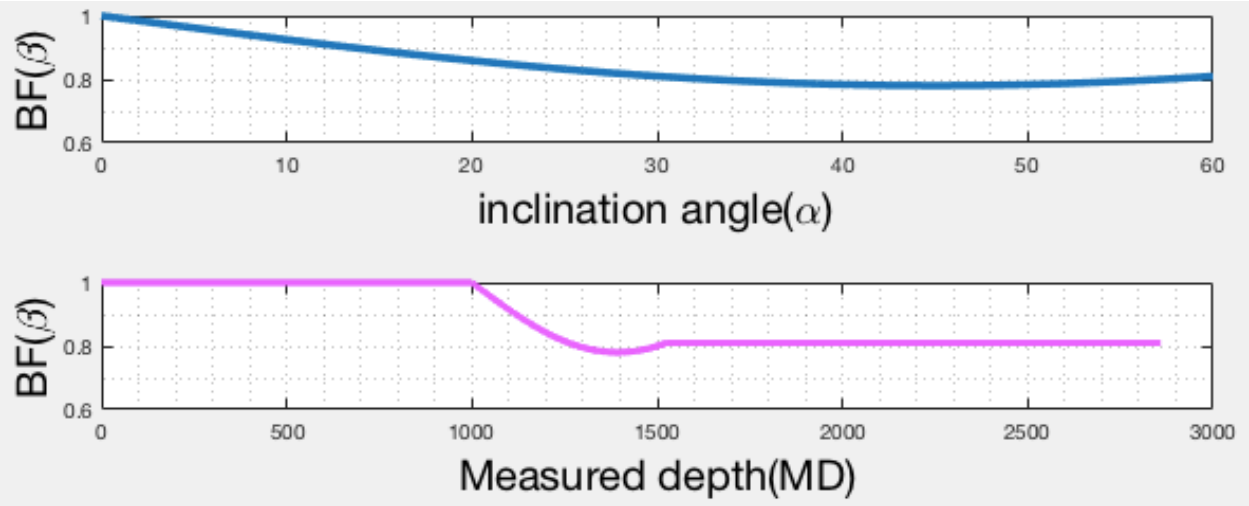

Figure 9-7: Buoyancy factor in a deviated well

Figure 9-7 shows variation of buoyancy factor in a deviated well. The upper plot is the change in buoyancy factor with inclination while the upper plot presents change in buoyancy factor over the measured depth. In both cases, buoyancy factor decreases with increase in inclination angle or depth. The lower plot reveals that buoyancy factor remains equal to 1 in a vertical section (i.e. from 0 to 1000 mMD) and starts decreasing as the inclination angle increases. At a certain angle, the buoyancy factor seems to increase again as the inclination angle exceeds 45°. However, this increase in buoyancy factor remains constant as the well path enters the tangent section where the inclination angle is constant over the entire tangential section. At such a high angle of inclination, the buoyancy factor remains as same as $1 - \left(\frac{\rho_{mud}}{\rho_{steel}}\right)$. In this particular example as given in the sample calculation, as the inclination angle reaches the maximum angle, the buoyancy factor is about 0.81 which is close to $1 - \left(\frac{\rho_{mud}}{\rho_{steel}}\right) = 1 - \left(\frac{1.5}{7.84}\right) = 0.8087$.

10.0 Weight on Bit(WOB) as a Kick Indicator

It is important to estimate and analyze weight on bit (DWOB) during drilling operation for the purpose of optimization. The use of correct weight on bit (WOB) is a key factor of drilling optimization to achieve an optimal rate of penetration (ROP). Weight on bit is directly linked to rate of penetration and drilling performance. Too low WOB might result in low ROP whereas too high WOB can result in a damaged drill bit. Therefore, obtaining actual downhole WOB is crucial in achieving good performance of a drill bit(Wu & Hareland, 2012).

In this chapter, real time drilling data (RTDD) such as hook load (HKL), measured bit depth (DBTM), measured hole depth (DMEA) and rotation of the drill string (RPM) are used as input to calculate WOB in two steps. The first step uses the difference in HKL when rotating off-bottom and when rotating on-bottom to calculate surface weight on bit (SWOB). The weight of the drill string is calculated in the second step, and iterations with different WOB values are performed until the calculated hook load matches the measured HKL with a small margin using torque and drag model.

10.1 DWOB vs. SWOB

While drilling, the weight cell installed in the BHA records the weight to the bit provided by the drill collars and this weight is known as downhole weight on bit. This weight is also known as the on-bottom weight on bit because it is recorded when the bit is on bottom. On the other hand, surface weight on bit is measured at the surface when the bit is off-bottom.

A programmed system can be used to determine when the bit is of bottom or on bottom. Normally, when the bit depth is within a certain range of well depth, the bit is on bottom. The bit is said to be off bottom when the bit depth is less than the measured depth. When off bottom, the weight recorded at the surface is the total weight of the drill string known as total hookload. Table 10-1 presents real time drilling data showing when the bit is on or off bottom. At about 1567.6m the bit approaches the bottom of the well and it is shown that, just before touching the bottom of the well at 1567.7m, hookload was 90.2tonnes which dropped to 87.92tonnes when the bit was on bottom. This shows that some weight of the drill string was taken by the bit and this difference in hookload

when the bit is off bottom and on bottom is the surface weight on bit. In this case, this was 2.28tonnes.

Table 10-1: Real - Time Drilling Data from 1567.7m to 1569.2m for Well 47-8-5

Hole Depth (m)	Bit Depth (m)	WOB (tonne)	HKL (tonne)	RPM (rev/min)	SPP (bar)	Torque (kNm)
1567.7	1566.1	0	90.25	80.43	144.26	13.42
1567.7	1566.3	0	90.38	80.61	144.11	13.09
1567.7	1566.6	0	90.54	80.63	143.97	12.52
1567.7	1566.8	0	90.54	80.65	144.04	12.64
1567.7	1567	0	90.39	80.62	143.81	13.56
1567.7	1567.4	3.59	90.13	80.54	144.46	14.63
1567.7	1567.6	3.51	90.2	80.45	144.37	14.17
1567.7	**1567.7**	**5.79**	**87.92**	**80.56**	**144.62**	**13.43**
1567.7	1567.7	9.32	84.4	80.66	144.71	14.03
1567.7	1567.7	11.42	82.3	80.67	144.57	14.83
1567.7	1567.7	12.09	81.63	80.58	143.84	14.93
1567.8	1567.8	12.86	80.85	80.57	144.42	15.81
1567.9	1567.9	12.19	81.53	80.66	145.44	17.26
1568	1568	12.51	81.2	80.58	145.26	17
1568.1	1568.1	14.71	79.01	80.51	145.54	17.42
1568.2	1568.2	17.32	76.4	80.36	146.05	20.16
1568.4	1568.4	17.25	76.47	80.64	145.99	18.69
1568.5	1568.5	12.47	81.24	80.59	145.93	17.73
1568.6	1568.6	12.17	81.54	102.46	145.88	16.22
1568.7	1568.7	12.12	81.6	102.35	145.66	16.16
1568.9	1568.9	17.56	76.16	102.31	145.94	18.07
1569	1569	18.27	75.44	102.34	146.16	17.19
1569.1	1569.1	20.5	73.22	102.22	146.63	22.44
1569.2	1569.2	21.03	72.69	102.34	146.46	21.2

The surface weight on bit is subjected to friction force and sometimes geometry of the well. This leads to difference in surface weight on bit and downhole weight on bit. If the bulk density in the well does not change, then the two must be the same assuming that friction is negligible since the bit is off bottom rotating. Also if density changes, the values must change and this change in surface and downhole weight on bit can be used to anticipate the onset of a kick at the bottom.

Therefore, it is very important to be sure that the weight on bit given by the weight cell is accurate and reliable so that any deviation of weight on bit from the surface weight on bit is correctly interpreted as change in the downhole conditions. An abrupt increase in downhole weight on bit would indicate a low density fluid entered the wellbore while an abrupt increase in surface weight on bit while pooling out of the hole would indicate more opposing forces in the well such as friction forces along the drill string.

10.2 Estimation of DWOB from SWOB

Surface weight on bit can be calculated from real time drilling data when the bit is off bottom rotating. The difference between hookload when the bit is off bottom and that when the bit is on bottom gives surface weight on bit given as:

$$\text{SWOB} = \text{HKL}_{\text{offbottom}} - \text{HKL}_{\text{onbottom}} = \text{THKL} - \text{HKL} \tag{10.1}$$

Where THKL is the total hookload when bit is off bottom and HKL is the hookload when bit is on bottom. Surface weight on bit is always greater than the downhole weight on bit. The main reason why downhole weight on bit may be different from surface weight on bit is that downhole weight on bit is not affected by frictional forces acting on the drill string since it is measured at the bottom.

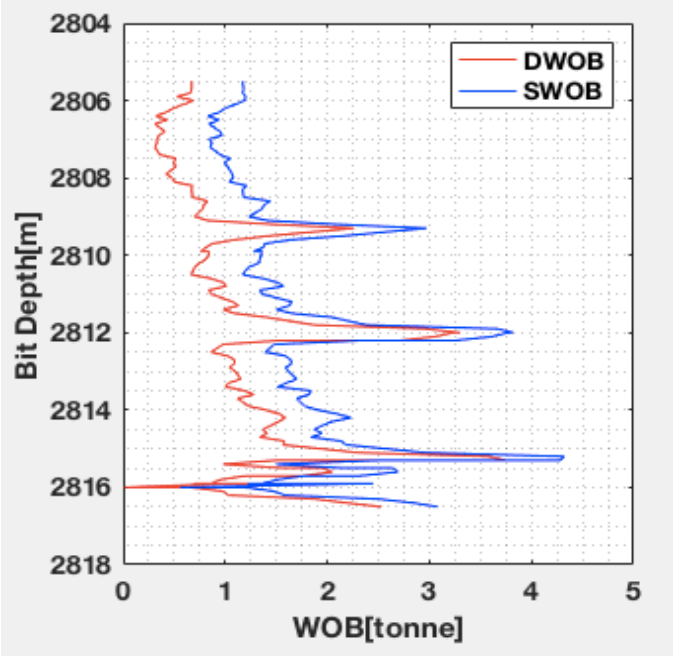

Figure 10-1: DWOB/SWOB vs. Bit depth

Figure 10-1 shows comparison between downhole and surface weight on bit for well 47-8-5. The surface weight on bit was calculated from hookload values when the bit was on and off bottom rotating. The results indicate that surface weight on bit is always greater than downhole weight on bit. The trend increases down the hole and at some depths such as 2809m, 2812m and 2815m both surface and downhole weight on bit increased rapidly. This may indicate change in bulk density at the bottom around the BHA which led to increase in both DWOB and SWOB.

10.2.1 *Converting SWOB into DWOB*

Friction needs to be taken into account in order to accurately calculate downhole weight on bit from the surface weight on bit so that the computed values match the measured downhole weight values. This can be done using two approaches, the torque and drag model and the finite element model. The torque and drag is simple and fast but does not give accurate results as finite element does. In this thesis, only torque and drag model was used to analyze the steps needed to estimate the downhole weight on bit under assumption that the wellbore section was straight. The torque and drag model for a straight section is given by:

$$F_k = \beta_k \, w dL_k \cos\alpha_i \pm \mu \, w dL_k \sin\alpha_i \tag{10.2}$$

Where F_i is the force at the top of element i and β_k is the buoyancy factor on element i. The second term in equation(10.2) is the frictional force, given by $Fr = \mu \, wdL\sin\alpha_i$ where μ is the coefficient of friction, w is the unit weight of the drill string element, dL_k is its length and α_i is the inclination angle.

Equation(10.2) can be used to estimate the frictional forces and finally the coefficient of friction using real time drilling data for when the bit is being pulled out of hole and when is being lowered into the hole. The pull up force is given by $F_{up} = \beta_k \, w dL_k \cos\alpha_i + \mu \, w dL_k \sin\alpha_i$ and when lowering into the well the force is given by $F_{down} = \beta_k \, w dL_k \cos\alpha_i - \mu \, w dL_k \sin\alpha_i$. Combining the two equations for F_{up} and F_{down} gives:

$$2\mu \, w dL_k \sin\alpha_i = Fr = F_{up} - F_{down} \tag{10.3}$$

Equation(10.3) can be converted into coefficient of friction as:

$$\mu = \frac{F_{up} - F_{down}}{2\, wdL_k \sin \alpha_i} \tag{10.4}$$

Equation(10.3) gives the frictional force from hookload values when the string is pulled out and when it is lowered into the well. This frictional force can be used to adjust the surface weight on bit through iterations until the difference between the measured and calculated downhole weight on bit is within acceptable range.

Table 10-2: RTDD during tripping operation for well 47-8-5

Hole Depth (m)	Bit Depth (m)	Motion	WOB (tonne)	HKL (tonne)	RPM (rev/min)	SPP (bar)
1579.8	1579.3	On bottom	17.94	83.78	120.54	146.81
1579.8	**1578.8**	Off bottom	**0**	**89.07**	**120.4**	**148.07**
1579.8	1578.1	up	0	90.65	120.59	147.68
1579.8	1577.7	up	0	87.78	120.6	148.57
1579.8	1577.2	up	0	87.24	120.63	148.56
1579.8	1576.8	up	0	87.17	120.65	148.03
1579.8	1573.5	up	0	89.43	41.91	2.38
1579.8	1574	up	0	89.47	42.11	149.04
1579.8	1574.6	down	0	89.45	42.11	98.26
1579.8	1575	down	0	89.34	42.09	126.93
1579.8	1576.4	down	0	89.23	42.13	143.92
1579.8	1577.1	down	0	89.19	42.17	148.56
1579.8	1579.8	On bottom	4.06	89.12	120.65	147.75

10.2.2 *Steps in Calculating DWOB from SWOB*

Table 10-2 shows real time drilling data when the drill string is off bottom. The frictional force for this depth interval can be calculated using equation(10.3). In this case F_{up}= 90.65tonnes while F_{down}= 89.43tonnes and frictional force is F_r = 1.05tonnes. Also the off bottom and on bottom hookload are 89.07 and 83.78tonnes respectively. This gives the surface weight on bit of

5.29tonnes while the downhole weight on bit is 4.06tonnes. This SWOB of 5.29tonnes is greater than DWOB by 1.23tonnes. This value is also greater than the calculated frictional force which is 1.05tonnes. After that a coefficient of friction needs to be calculated using equation(10.4) to re – estimate the new frictional force through iterations until when the surface weight on bit and downhole weight on bit differ by the frictional force calculated from the difference between the force during pulling up and the force during pulling down.

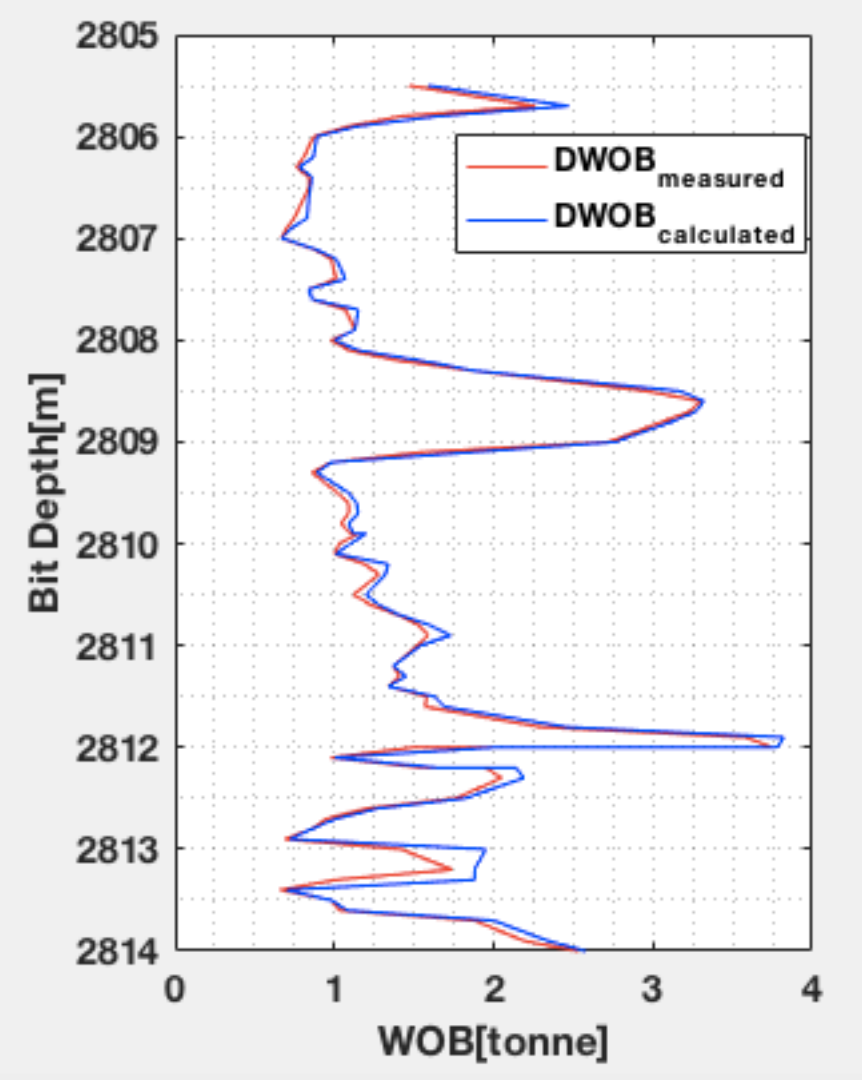

Figure 10-2: Measured and calculated downhole weight on bit

Figure 10-2 shows the estimated from RTDD for the depth interval of 2805m to 2814m. These downhole weight on bit were calculated using the procedures described in 10.2.2 above. The calculated DWOB matches the measured weight on bit with a small difference. It is shown that,

with all the small differences between the measured and calculated weight on bit values, the general trend between the two data sets remains identical.

10.3 Mud Weight and Buoyancy Factor from DWOB

Bulk density of the mud can be calculated from downhole weight on bit calculated from real time drilling data. The estimated DWOB is converted into buoyancy factor β given as:

$$\beta_k = \frac{DWOB_k}{wdL_k \cos \alpha_i} \tag{10.5}$$

Where β_k and $DWOB_k$ are the buoyancy factor and downhole weight on bit respectively at the k^{th} bit depth. This buoyancy factor can be converted into bulk density rho_{mud}, of the mud just below the bit using: Where rho_{mud} is the bulk density and rho_{steel} is density of steel.

$$rho_{mud} = (1 - \beta_k) rho_{steel} \tag{10.6}$$

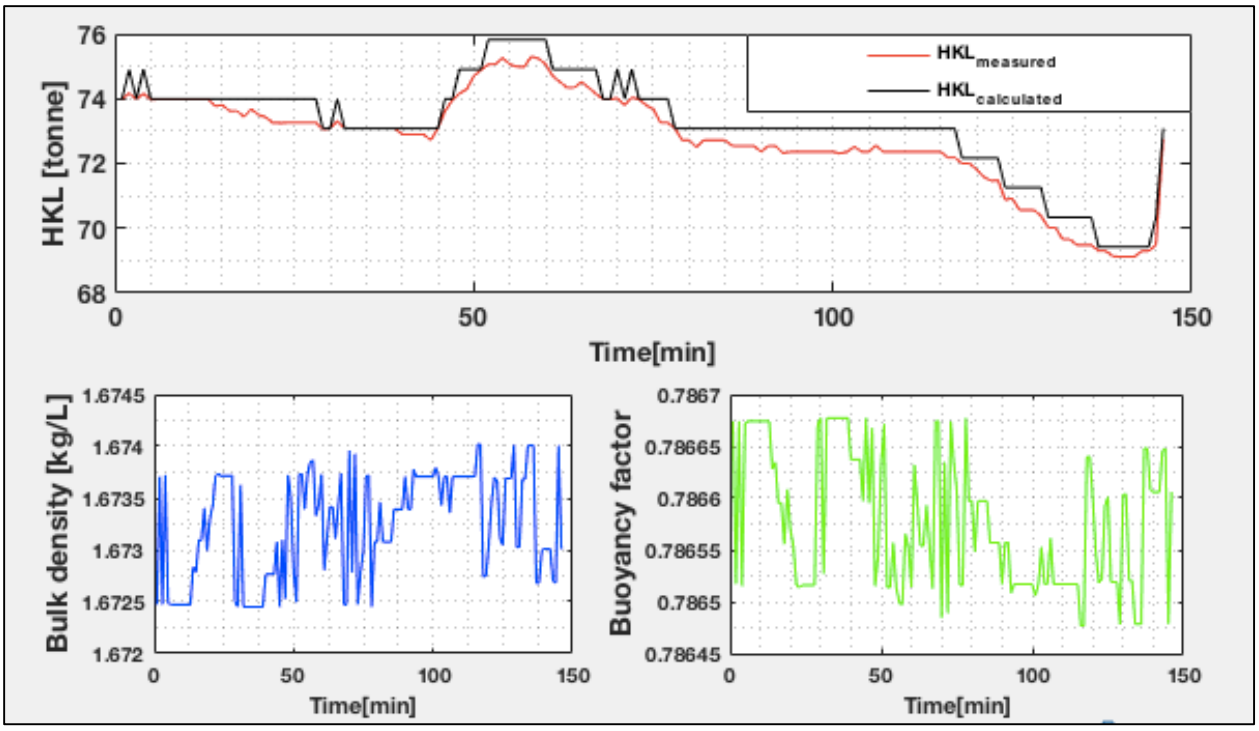

Figure 10-3: Hookload, density and buoyancy factor calculated from DWOB

Figure 10-3 shows drilling parameters calculated from downhole weight on bit. The upper plot is hookload calculated iteratively from downhole weight on bit. The lower plots present bulk density and the corresponding buoyancy factor. The plots show how bulk density and buoyancy factor are sensitive to change in hookload. Every time hookload changes leads to a corresponding change in bulk density and buoyancy factor. However, in the upper plot, the calculated hookload is a bit large than the measured hookload. This small discrepancy may be due to the torque and drag model which was used to calculate downhole weight. Although this method is fast, its accuracy depends on many assumptions like well geometry and hole condition. In this thesis, calculations of hookload were based on assumptions that the selected depth interval was in a straight section inclined at 30° and also friction and wall contact forces were ignored. For that reason, only friction in the well was taken into account. This might have been the reason why calculated hookload values were a bit greater than measured hookload values.

11.0 Conclusion and Recommendations

11.1 Conclusion

- Mathematical kick models have been developed. Drilling parameters which can change with changing downhole conditions have been investigated to show the dependence between them. Mud weight and buoyancy factor have been found to depend on gas fraction, cuttings concentration and temperature. Gas fraction in the mud has greater impact on mud weight than any other parameter in bottomhole pressure reduction while cuttings have less impact and normally leads to increase in mud weight.
- Mathematical models taking into account well geometry and a realistic drill string geometry were developed to estimate surface hookload. The Archimedes buoyancy model and the Piston – force model were compared and both were found to give approximately the same results although the Archimedes model was found to be more accurate.
- Downhole weight on bit model was developed whose inputs were surface hookload to calculate surface and downhole weight on bit. The calculated downhole weight on bit were close to measured downhole weight on bit. Discrepancies between the calculated and measured downhole weight on bit were due to use of the torque and drag model which is less accurate due to being affected by friction in the well. Bulk density and buoyancy factors calculated from downhole weight on bit were also found to sensitively change with change in surface hookload.
- Kick model based on downhole weight on bit would be more accurate and quick to give information at the surface about change in downhole conditions since downhole weight on bit gives a better estimate of mud weight because it is not affected by friction.
- It is difficult to say that models developed meet all requirements of being used to accurately predict the occurrence of a kick. The models were based on many assumptions and simplifications. However, based on these facts the most critical parameters of kick detection were established. A more general and realistic model which can take into account all parameters at the same time need to be developed. This can be a more realistic and accurate model to predict the presence of kick in the well.

11.2 Recommendations

- Wellbore and drill string geometry should be taken into account when estimating downhole weight on bit. Coefficient of friction should be accurately estimated in order to get correct weight on bit from surface weight on bit.
- Finite element method should be used to accurately estimate downhole weight on bit from surface hookload values since it might be accurate than the analytical torque and drag model. The model should be able to take into account the geometry of the wellbore.
- Real time drilling data from different wells should be used to test the downhole weight on bit model in order to validate the model.

References

Aadnøy, B. (2006) Mechanics of drilling. *Aachen: Shaker Verlag*, 196.

Aadnoy, B. S. & Djurhuus, J. (2008) Theory and Application of a New Generalized Model for Torque and Drag, 2008/1/1/. SPE: Society of Petroleum Engineers.

Aadnoy, B. S. & Huusgaard, P. P. (2002) Analytical Models for Design of Wellpath and BHA, 2002/1/1/. SPE: Society of Petroleum Engineers.

Aadnoy, B. S. & Kaarstad, E. (2006) Theory and Application of Buoyancy in Wells, 2006/1/1/. SPE: Society of Petroleum Engineers.

Aadnoy, B. S., Larsen, K. & Berg, P. C. (1999) Analysis of Stuck Pipe in Deviated Boreholes, 1999/1/1/. SPE: Society of Petroleum Engineers.

Bush, D. C. & Freeman, D. L. (1986) Drill Cuttings Porosity, Grain Density, And Permeability By Direct Laboratory Measurements And Their Relatability, 1986/1/1/. SPWLA: Society of Petrophysicists and Well-Log Analysts.

Farah, O. F. (2013) Directional well design, trajectory and survey calculations, with a case study in fiale, asal rift, djibouti, [Lecture]. Ministry of Energy and Natural Resources, unpublished.

Ford, J. T., Peden, J. M., Oyeneyin, M. B., Gao, E. & Zarrough, R. (1990) Experimental Investigation of Drilled Cuttings Transport in Inclined Boreholes, 1990/1/1/. SPE: Society of Petroleum Engineers.

Glomstad, T. S. (2012) *Analysis of Hook load Signal to reveal the Causes of Restrictions*Master's thesis. Norwegian University of Science and Technology, 4.6.201220.11.2016].

Goldsmith, R. (1972) Why gas cut mud is not always a serious problem. *World Oil*, 175(5), 51-+.

Gupta, V., Dhameliya, J. D. & Jain, S. (2013) Liquid Lift Dual Gradient Drilling in Deep Water: Early Kick Detection and Control, 2013/4/19/. SPE: Society of Petroleum Engineers.

Hollman, L., Haq, I., Christenson, C., Silva, T. P. d., Fayed, M. I. B., Thorn, N. & Geldof, W. (2016) Developing a MPD Operation Matrix – Case History, 2015/3/17/. SPE: Society of Petroleum Engineers.

Hovda, S. (2017) Semi-analytical models on axial motions of an oil-well drillstring, Part II: Deviated wellbores, S.P Andersens veg 15a, Trondheim Norway.

Jonathan Felipe Galdino, Gabriel Merhy de Oliveira, Admilson T. Franco & Negrão, C. O. R. (2013) Transient Mathematical Model for Well Kick During Drilling Operations

Kristensen, E. (2013) *Model of Hook Load During Tripping Operation*Master's thesis. Norwegian University of Science and Technology, June19.11.2016].

Ling, K., He, J., Ge, J., Pei, P. & Shen, Z. (2015) A rigorous method to calculate the rising speed of gas kick. *Journal of Petroleum Exploration and Production Technology*, 5(1), 81-89.

Lockett, T. J., Richardson, S. M. & Worraker, W. J. (1993) The Importance of Rotation Effects for Efficient Cuttings Removal During Drilling, 1993/1/1/. SPE: Society of Petroleum Engineers.

McCann, R. C., Quigley, M. S., Zamora, M. & Slater, K. S. (1995) Effects of High-Speed Pipe Rotation on Pressures in Narrow Annuli.

Ozbayoglu, M. E., Saasen, A., Sorgun, M. & Svanes, K. (2008) Effect of Pipe Rotation on Hole Cleaning for Water-Based Drilling Fluids in Horizontal and Deviated Wells, 2008/1/1/. SPE: Society of Petroleum Engineers.

Rader, D. W., Bourgoyne, A. T., Jr. & Ward, R. H. (1975) Factors Affecting Bubble-Rise Velocity Of Gas Kicks.

Rommetveit, R., Fjelde, K. K., Aas, B., Day, N. F., Low, E. & Schwartz, D. H. (2003) Hpht well control; an integrated approach, *Offshore Technology Conference*. Offshore Technology Conference.

Saasen, A. (1998) Hole Cleaning During Deviated Drilling - The Effects of Pump Rate and Rheology, 1998/1/1/. SPE: Society of Petroleum Engineers.

Sifferman, T. R. & Becker, T. E. (1992) Hole Cleaning in Full-Scale Inclined Wellbores.

Skalle, P. (2015a) *Drilling Fluid Engineering*, 6th edition.

Skalle, P. (2015b) *Pressure Control During Oil Well Drilling*, 6th edition.

Skalle, P., Podio, A. L. & Tronvoll, J. (1991) Experimental Study of Gas Rise Velocity and tis Effect on Bottomhole Pressure in a Vertical Well *Offshore Europe Conference.* Aberdeen.

Stokka, S. I., Andersen, J. O., Freyer, J. & Welde, J. (1993) Gas Kick Warner - An Early Gas Influx Detection Method, 1993/1/1/. SPE: Society of Petroleum Engineers.

Strong, M. W. (1939) Mud Technique in Iran.

Swanson, B. W., Gardner, A. G., Brown, N. P. & Murray, P. J. (1997) Slimhole Early Kick Detection by Real-Time Drilling Analysis.

Velmurugan, N., Bansal, G. & Sharma, T. (2015) WellCON: Early Kick Detection System Extended to Kill Sheet, 2015/12/6/. IPTC: International Petroleum Technology Conference.

Wold, A. A. & Kummen, H. T. (2015) *The effect of cuttings on annular pressure loss-An analysis of field data in the North Sea*NTNU.

Wu, A. & Hareland, G. (2012) Calculation of Friction Coefficient And Downhole Weight On Bit With Finite Element Analysis of Drillstring, 2012/1/1/. ARMA: American Rock Mechanics Association.